

How fluid-rock interactions and fabric development affect friction: towards a microphysical basis for Rate-and-State Friction

Sabine den Hartog
Pennsylvania State University
U.S.A.
s.denhartog@psu.edu



André Niemeijer
Utrecht University, HPT Laboratory
The Netherlands
a.r.niemeijer@uu.nl



European Research Council
Established by the European Commission



Universiteit Utrecht

NWO
Netherlands Organisation
for Scientific Research

Outline

1. History and background of rate-and-state friction (RSF)
2. Fault-scale modeling using RSF
3. Physical interpretations of RSF
4. Variation of friction with active foliation development and fluid-rock interactions – analogue experiments and models
5. Experiments on real fault gouge materials & model

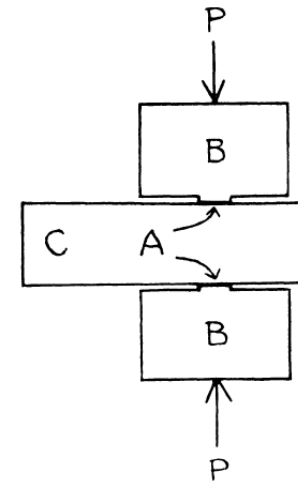
Some history

THE JOURNAL OF GEOLOGY

August-September 1936

SHEARING PHENOMENA AT HIGH PRESSURE OF
POSSIBLE IMPORTANCE FOR GEOLOGY

P. W. BRIDGMAN



These rupture phenomena may or may not be superposed on the ordinary phenomena of plastic flow. Thus there are substances, of which graphite is a conspicuous example, which show no trace of plastic flow; rupture occurs, there is a jump in angular displacement and a jump down in the force, the force then builds up again with practically no further increase in angular displacement until the critical force for rupture is reached, and the process repeats.

First description of rupture in the laboratory !

Experiments on a wide variety of materials using a rotary shear device

Some history

Stick-Slip as a Mechanism for Earthquakes

Abstract. *Stick-slip often accompanies frictional sliding in laboratory experiments with geologic materials. Shallow-focus earthquakes may represent stick-slip during sliding along old or newly formed faults in the earth. In such a situation, observed stress drops represent release of a small fraction of the stress supported by the rock surrounding the earthquake focus.*

- Brace & Byerlee (Science, 1966) propose that “stick-slips” are the laboratory equivalent of earthquakes.
- Friction as opposed to fracture

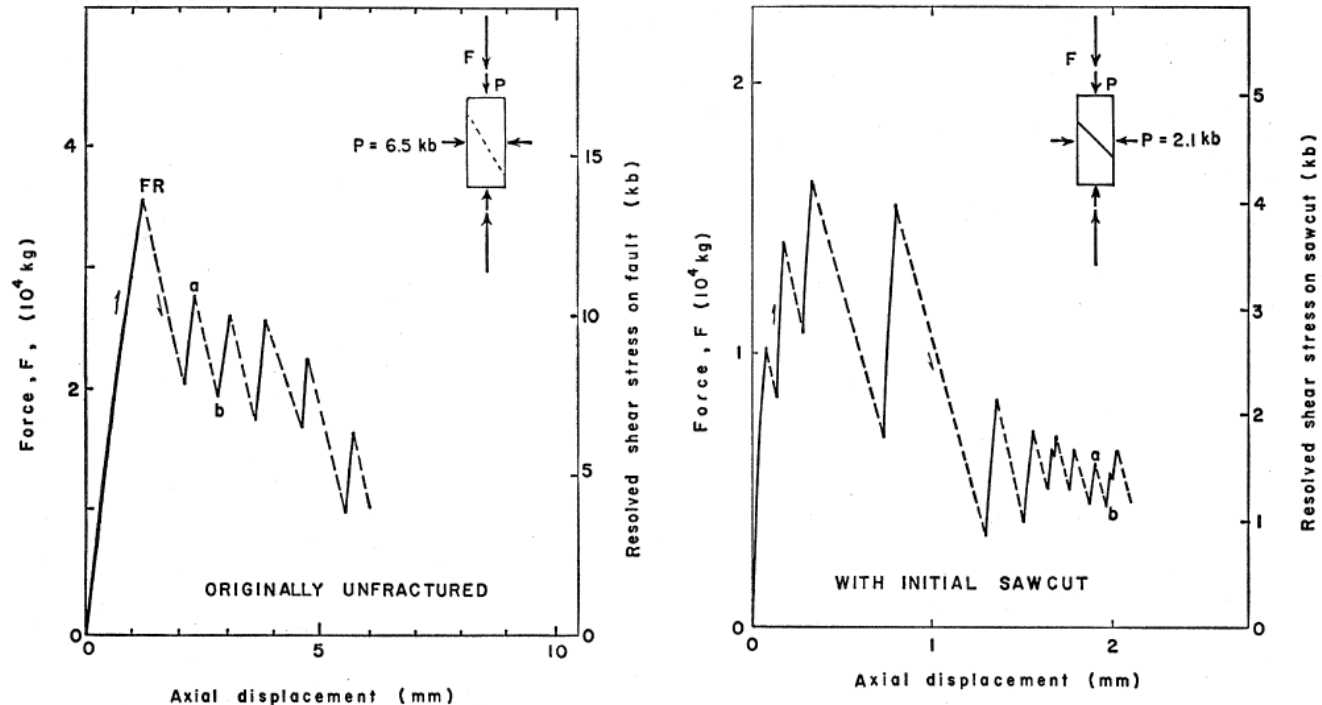


Fig. 1 (left). Force-displacement curve for the axial direction in a cylindrical sample of Westerly granite. Small diagram above the curve shows schematically how stress was applied to the sample. The sample fractured at point *FR* forming the fault which is shown as a dotted line in the small diagram. The exact shape of the curves during a stress drop (such as *ab*) is not known and is shown dotted. *P* is confining pressure. Fig. 2 (right). Same as Fig. 1 except that the sample contained a sawcut with finely ground surfaces as shown schematically (small figure) by a heavy line.

26 AUGUST 1966

991

Some history

Bulletin of the Seismological Society of America. Vol. 57, No. 3, pp. 341-371. June, 1967

MODEL AND THEORETICAL SEISMICITY

BY R. BURRIDGE AND L. KNOPOFF

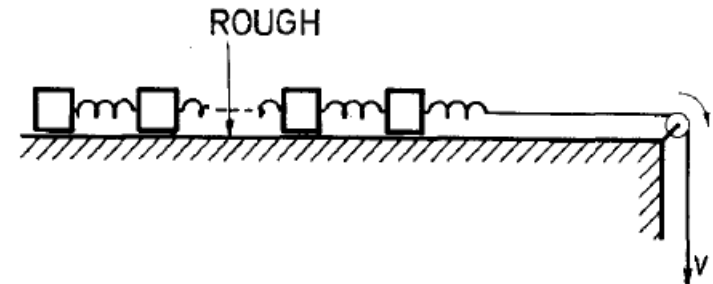
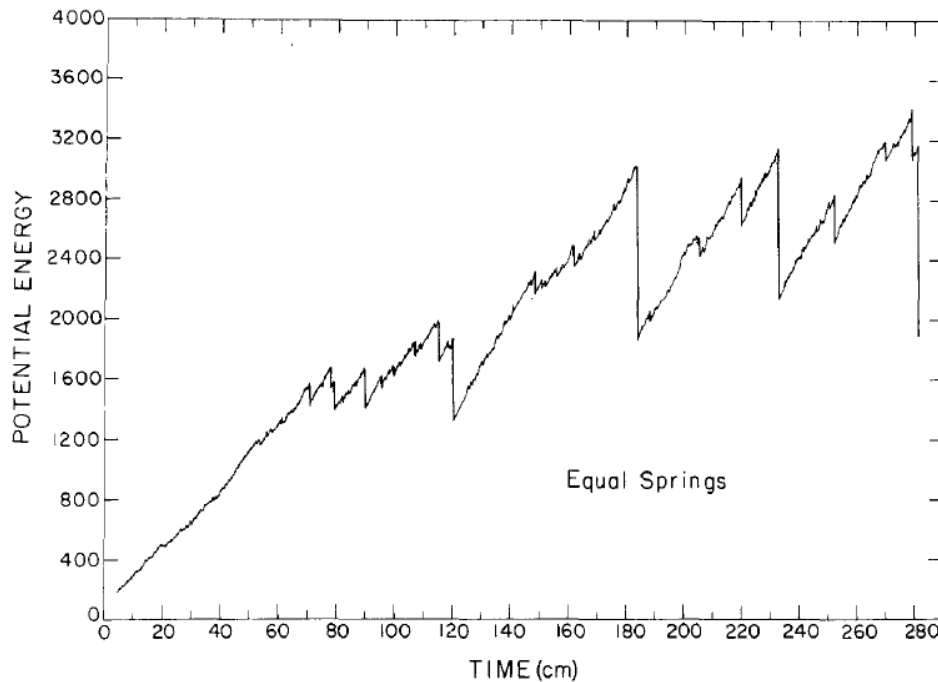


FIG. 3. Schematic diagram of the laboratory model.

- Spring-slider model generating quasi-periodic slip events
- EQ cycle controlled by friction

FIG. 4. Potential energy as a function of time for the mass-spring system with all springs equal.

Some history

VOL. 84, NO. B5

JOURNAL OF GEOPHYSICAL RESEARCH

MAY 10, 1979

Modeling of Rock Friction

1. Experimental Results and Constitutive Equations

JAMES H. DIETERICH

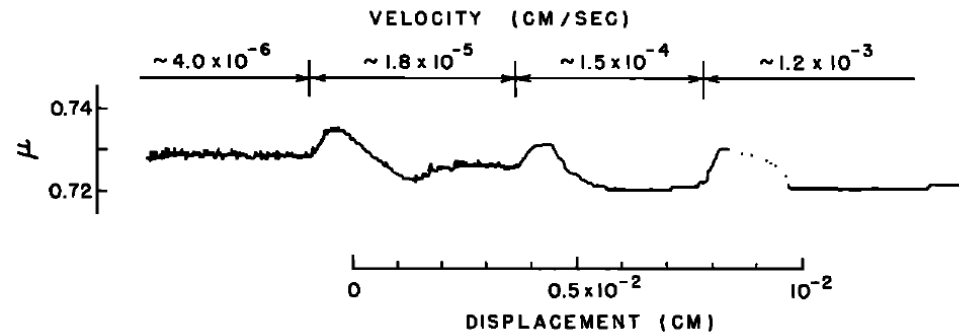


Fig. 1. Coefficient of friction μ versus displacement. Slip velocities are shown by the arrows above the experimental curves.

- Results from sliding experiments on granodiorite at 6.07 MPa and room T
- Velocity-dependence of friction result of time-dependence of contact area
- Formulation of time and displacement-dependent friction, initial form of rate- and state-friction equations (RSF)

Some history

JOURNAL OF GEOPHYSICAL RESEARCH, VOL. 88, NO. B12, PAGES 10,359–10,370, DECEMBER 10, 1983

Slip Instability and State Variable Friction Laws

ANDY RUINA

$$\tau = F(\sigma, V, \theta_1, \theta_2, \dots) \quad (3a)$$

$$d\theta_i/dt = G_i(\sigma, V, \theta_1, \theta_2, \dots) \quad i = 1, 2, \dots \quad (3b)$$

One hopes that for practical purposes the numbers of state variables θ_i required is small. The variables θ_i then represent some kind of average of an undoubtedly complicated surface state.

- Concept of state variables
- Formulation of RSF equations

Some history

JOURNAL OF GEOPHYSICAL RESEARCH, VOL. 88, NO. B12, PAGES 10,359–10,370, DECEMBER 10, 1983

Slip Instability and State Variable Friction Laws

ANDY RUINA

$$\tau = F(\sigma, V, \theta_1, \theta_2, \dots) \quad (3a)$$

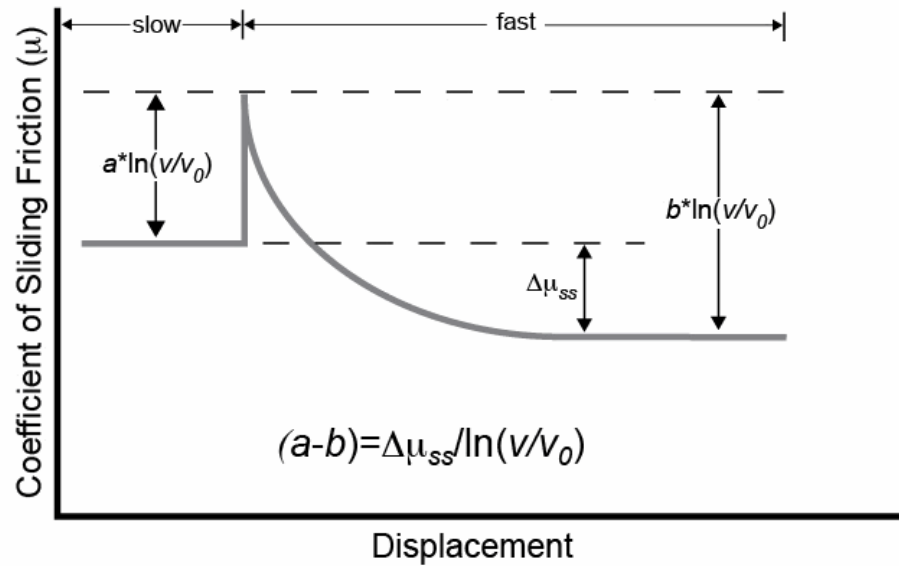
$$d\theta_i/dt = G_i(\sigma, V, \theta_1, \theta_2, \dots) \quad i = 1, 2, \dots \quad (3b)$$

One hopes that for practical purposes the numbers of state variables θ_i required is small. The variables θ_i then represent some kind of average of an undoubtedly complicated surface state.

- Concept of state variables
- Formulation of RSF equations

The usefulness of the state variable concept does not depend on physical interpretation of the state variables (like temperature or entropy in thermodynamics) though discovery of such interpretation would add tremendously to the credence and usefulness of the theory.

Rate and State friction equations



$$\mu = \mu_0 + a \cdot \ln\left(\frac{v}{v_0}\right) + b \cdot \ln\left(\frac{v_0 \theta}{d_c}\right)$$

$$\frac{d\theta}{dt} = 1 - \frac{V\theta}{d_c}$$

“Slowness law” or
“Dieterich-Ruina law”

$$\frac{d\theta}{dt} = -\frac{v\theta}{d_c} \ln\left(\frac{v\theta}{d_c}\right)$$

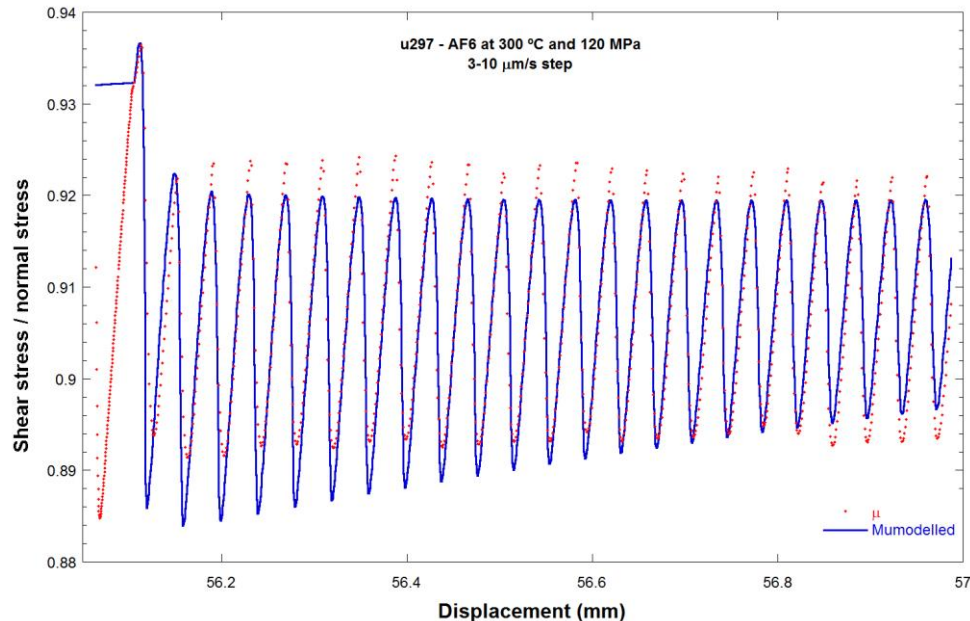
“Slip law” or
“Ruina law”

RSF - experiments

Coupling of RSF equations with an equation describing the interaction with the elastic loading frame

$$\frac{d\mu}{dt} = k(v_{lp} - v)$$

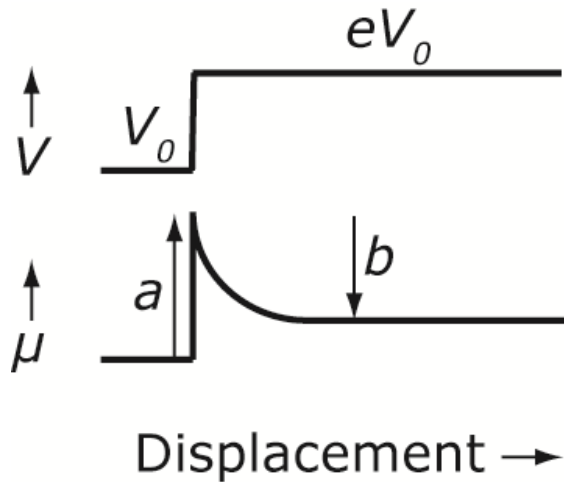
1. Solve for v gives the evolution of friction with time (displacement)
2. Invert for experimental data to obtain a , b and d_c



Stick-slip behaviour

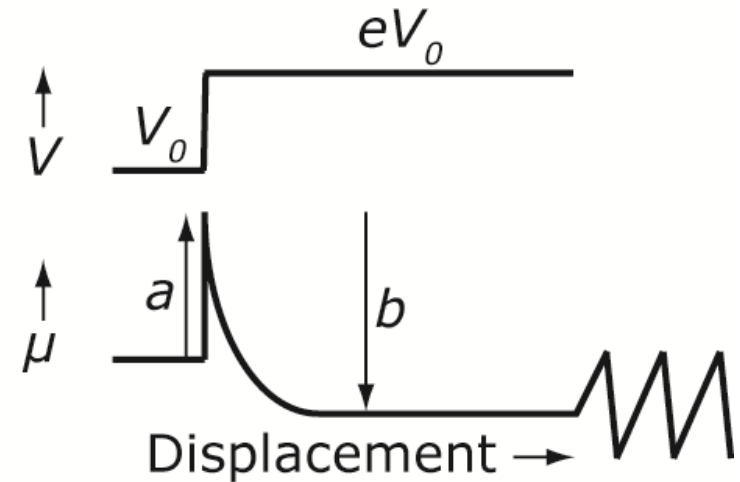
RSF – (a-b)

At steady state: $(a-b) = \frac{\Delta\mu_{ss}}{\ln(V/V_0)}$



$(a-b) \geq 0$
Velocity strengthening

Stable slip



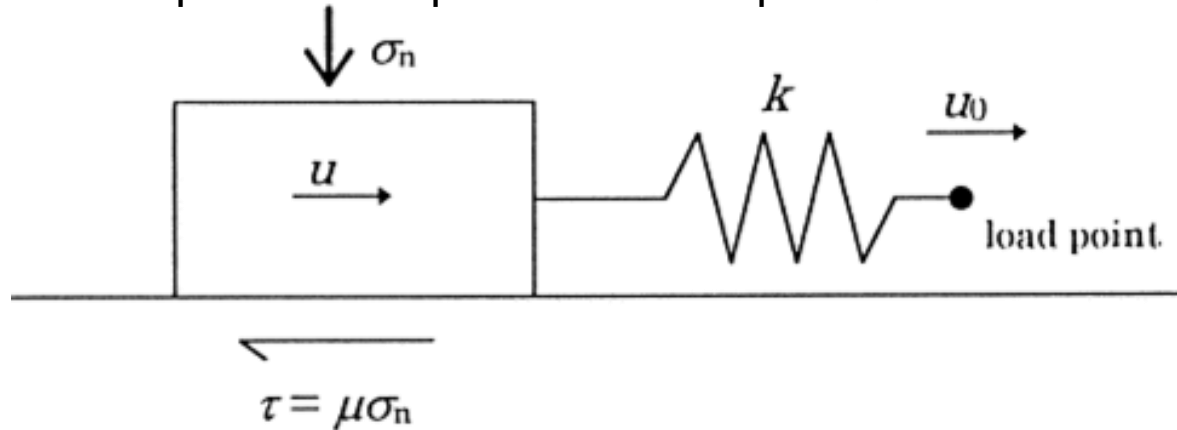
$(a-b) < 0$
Velocity weakening

Potentially unstable slip

RSF – seismic cycle

Spring-slider analogue

RSF equations coupled with the equation of motion



If $(a-b) > 0$, stable sliding

→ $V_{\text{block}} = V_{\text{spring}}$

If $(a-b) < 0$, unstable sliding possible

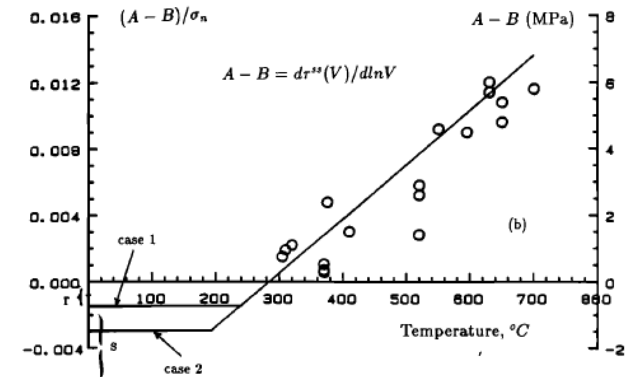
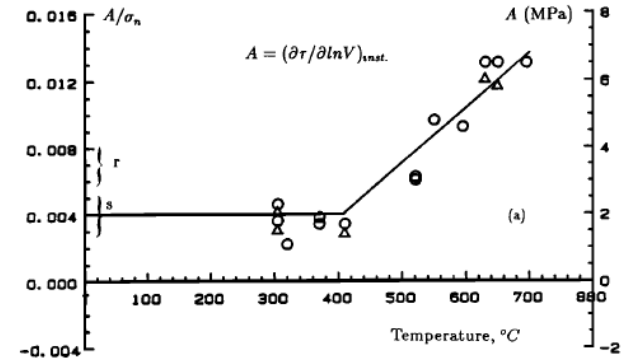
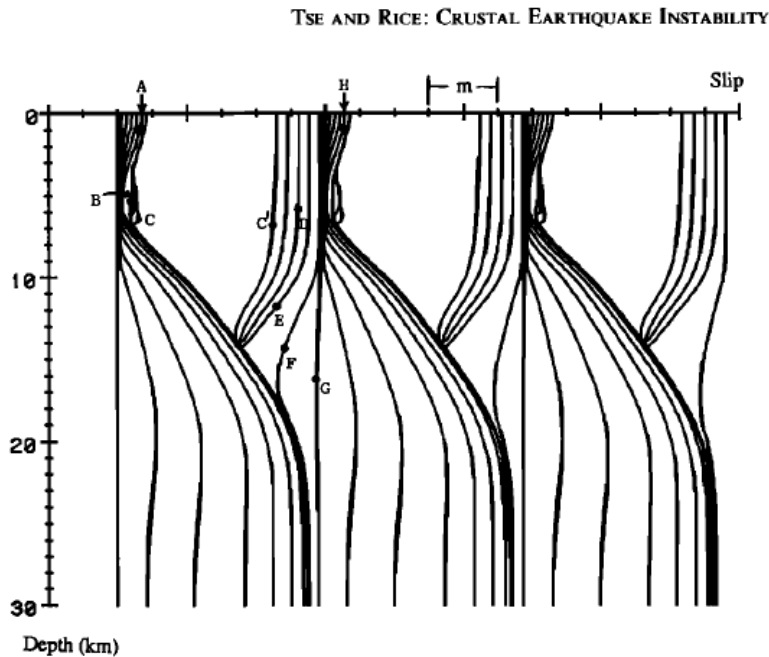
→ $V_{\text{block}} = 0$ until $F > \mu_{\text{static}} F_n$ → sudden drop in force and $V_{\text{block}} \gg V_{\text{spring}}$

Stability criterion: unstable slip when $\sigma > \sigma_c = \frac{Kd_c}{-(a-b)}$

RSF – seismic cycle simulation

Tse & Rice, JGR, 1986

(a-b) varies with temperature (depth)

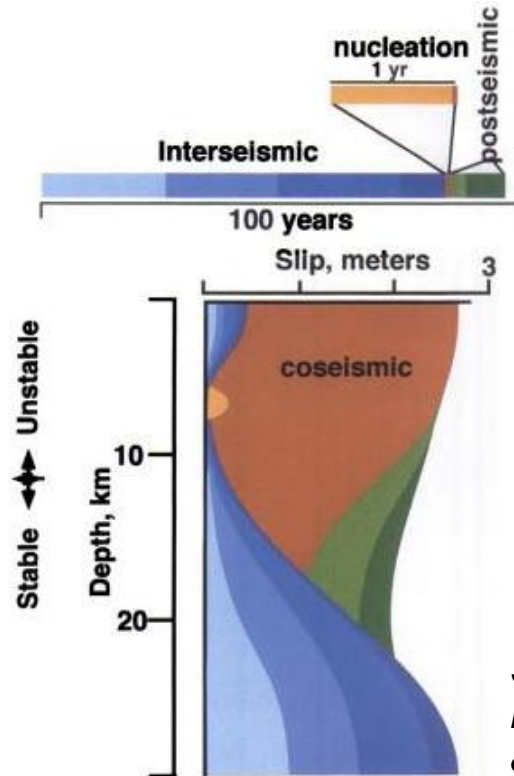


1. Simulations explain depth extent of seismicity
2. Nucleation occurs at depths of 3-7 km, which depends on only mild variations in the constitutive parameters

RSF – seismic cycle simulation

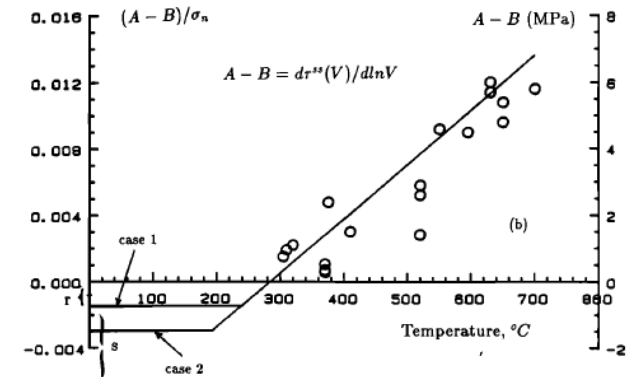
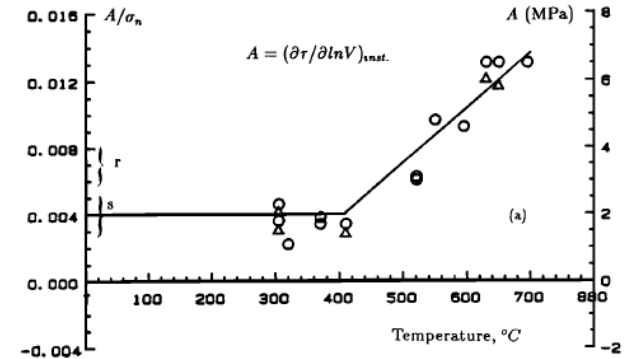
Tse & Rice, JGR, 1986

(a-b) varies with temperature (depth)



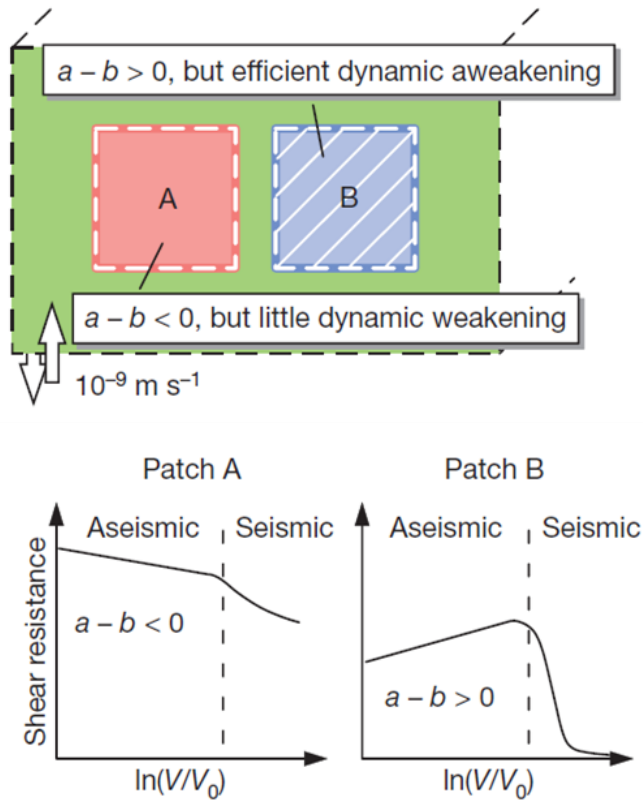
Scholz (2002)
Modified from Tse
& Rice (1986)

1. Simulations explain depth extent of seismicity
2. Nucleation occurs at depths of 3-7 km, which depends on only mild variations in the constitutive parameters



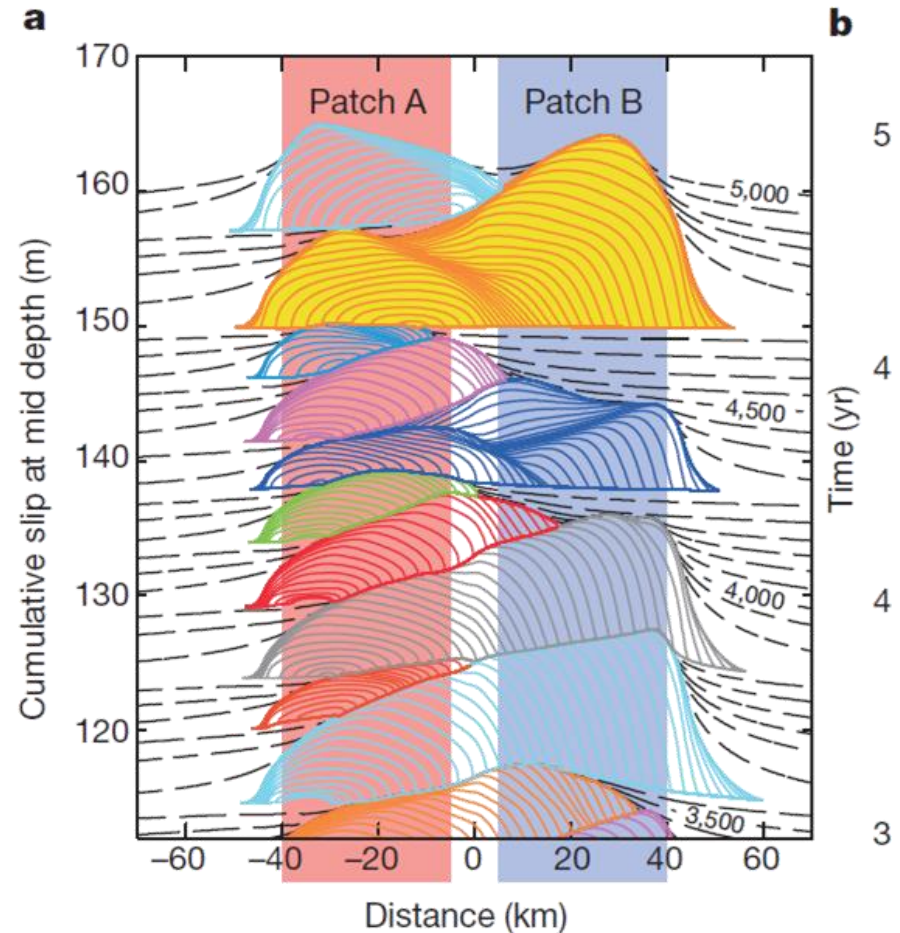
RSF – seismic cycle simulation

Noda and Lapusta, Nature, 2013



Variation in (a-b) with sliding velocity

Enhanced weakening at seismic velocities allows propagation of seismic slip in velocity-strengthening material.



RSF – seismic cycle simulation

Many more examples, e.g.

- Weeks, JGR, 1993, effect of positive (a-b) at high velocities on earthquake stress drop
- Dieterich, JGR, 1994, earthquake clustering (aftershocks)
- Boatwright and Cocco, JGR, 1996, effect of spatial distribution of (a-b) on earthquake size
- Kaneko et al, Nature Geoscience, 2010, effect of the presence of stable (positive (a-b) patch on earthquake size

Interpretation of Rate-and State

Baumberger et al. (1999) rewrote RSF as:

$$F = s(V)A_r(\theta)$$

with

$$A_r(\theta) = A_0 \left[1 + \beta \ln \left(\frac{\theta V_0}{D_c} \right) \right] \quad (1)$$

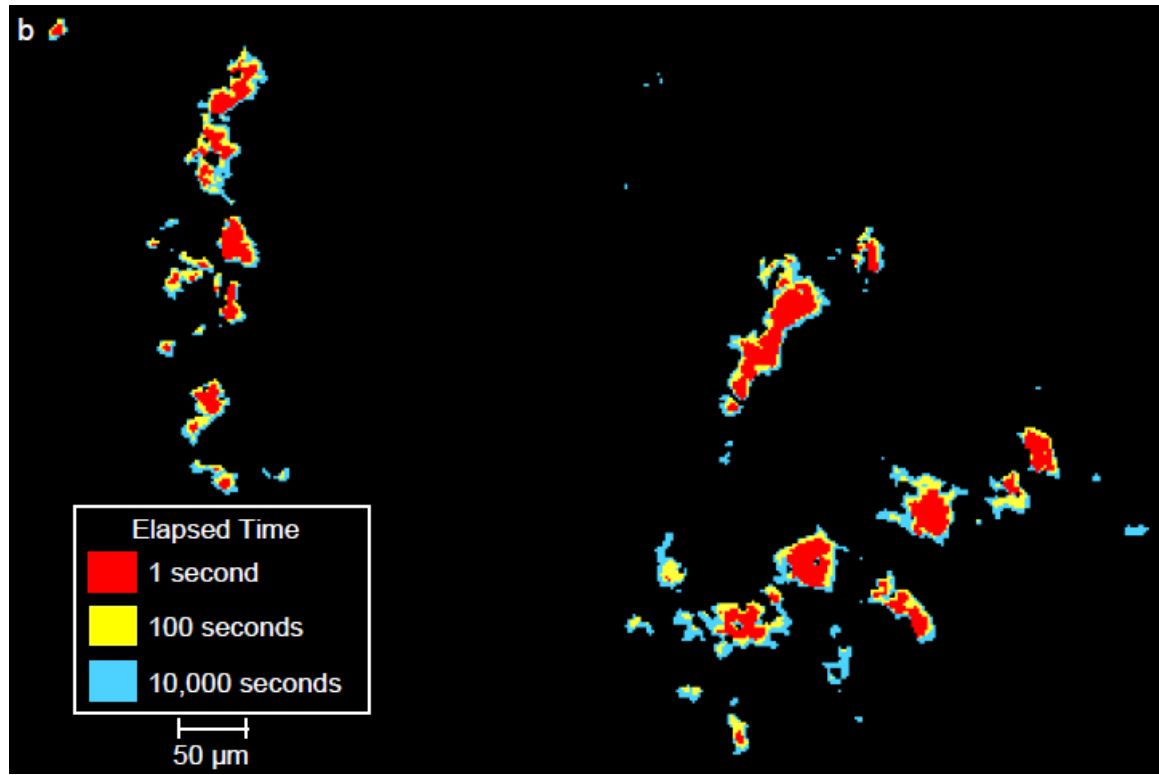
and

$$s(V) = s_0 \left[1 + \alpha \ln \left(\frac{V}{V_0} \right) \right] \quad (2)$$

Equation (1) represents the increase of real area of contact with (log) contact time

Equation (2) represents the velocity dependence of contact shear strength

Interpretation of Rate-and State



Dieterich & Kilgore, Pageoph, 1994

Growth of real area of contact under stationary load

- Attributed to “asperity creep”
- Occurs only in the presence of water (vapor)
- Underlying mechanism(s) unclear
- Mechanism probably varies with P,T, H₂O-content/composition

Interpretation of Rate-and State

Velocity dependence of contact shear strength has been argued to be due to a form of thermally activated anelastic shear creep at contact junctions (Baumberger et al. 1999, Nakatani, 2001, Scholz, 2002):

$$s(V, T) = \frac{kT}{\Omega} \left[\ln \left(\frac{V}{V_0} \right) + \frac{Q}{kT} \right]$$

with Ω and Q the activation volume and energy, respectively

→ Actual deformation mechanism still not defined – how to extrapolate ?

- Beeler et al. (JGR, 2007) showed that for weak phyllosilicates (serpentinite and talc), a can be directly (and quantitatively) related to the strain dependence of **dislocation glide**.
- However, a similar approach could not quantitatively link the direct effect to the rate dependence of subcritical crack growth in granitic or quartz-rich rocks.

Importance of a 3D-volume vs. slip on an interface → contribution of volume changes to friction (shear stress)

Interpretation of Rate-and State

Importance of a 3D-volume vs. slip on an interface → contribution of volume changes to friction (shear stress)

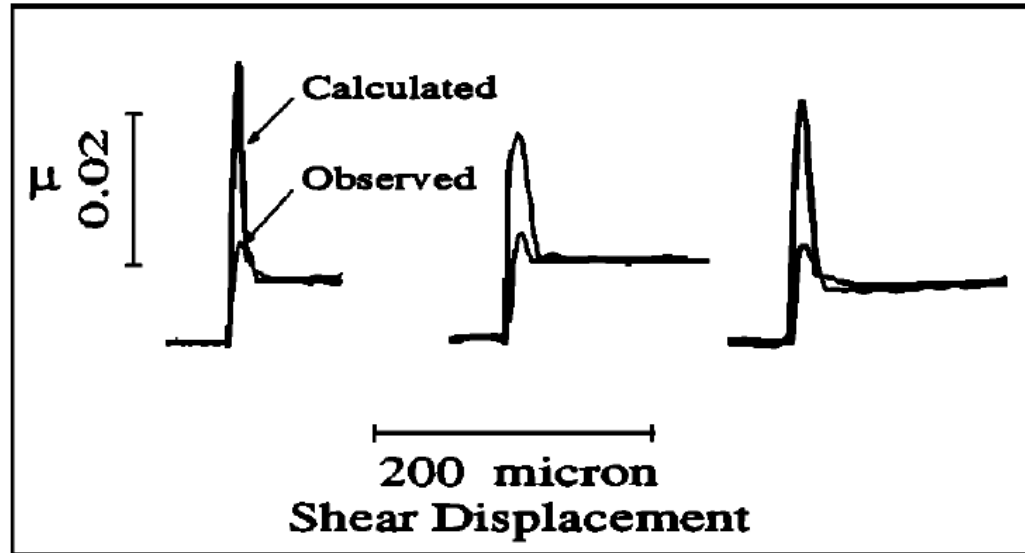


Fig. 22. Calculated and observed friction over three velocity steps assuming (1) an intrinsic steady state velocity weakening term of -0.002 ($a-b$) for μ_f and (2) that transient slip occurs at 15° to the gouge layer. The calculated curve was derived using equation (7) with normal stress increasing linearly from $(0.65 \sigma')$ to σ' over the

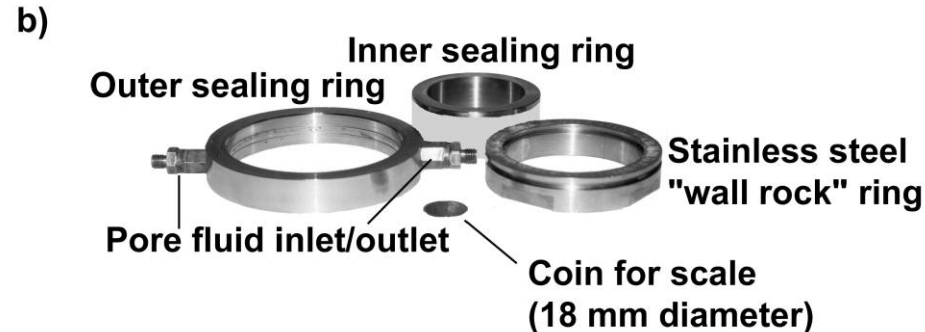
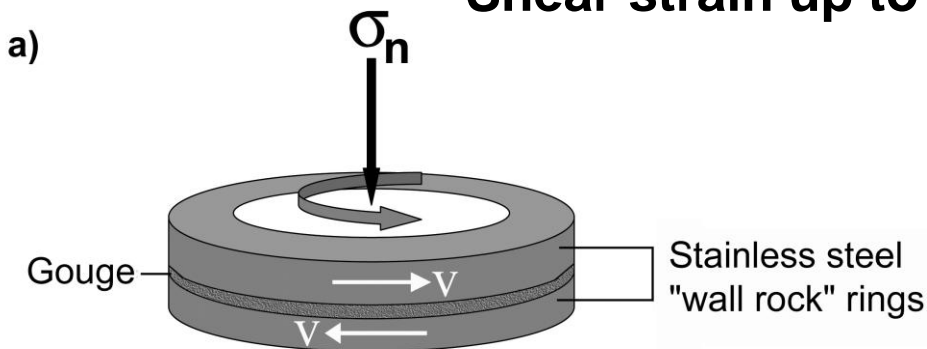
- Marone et al, JGR, 1990 showed that dilatancy significantly affects observed a
 - Depends on sliding history (displacement), grain size, localization, etc.
- See also Sammis and Steacy, *Pageoph*, 1994 and other work by Sammis and co-workers

Interpretation of Rate-and State

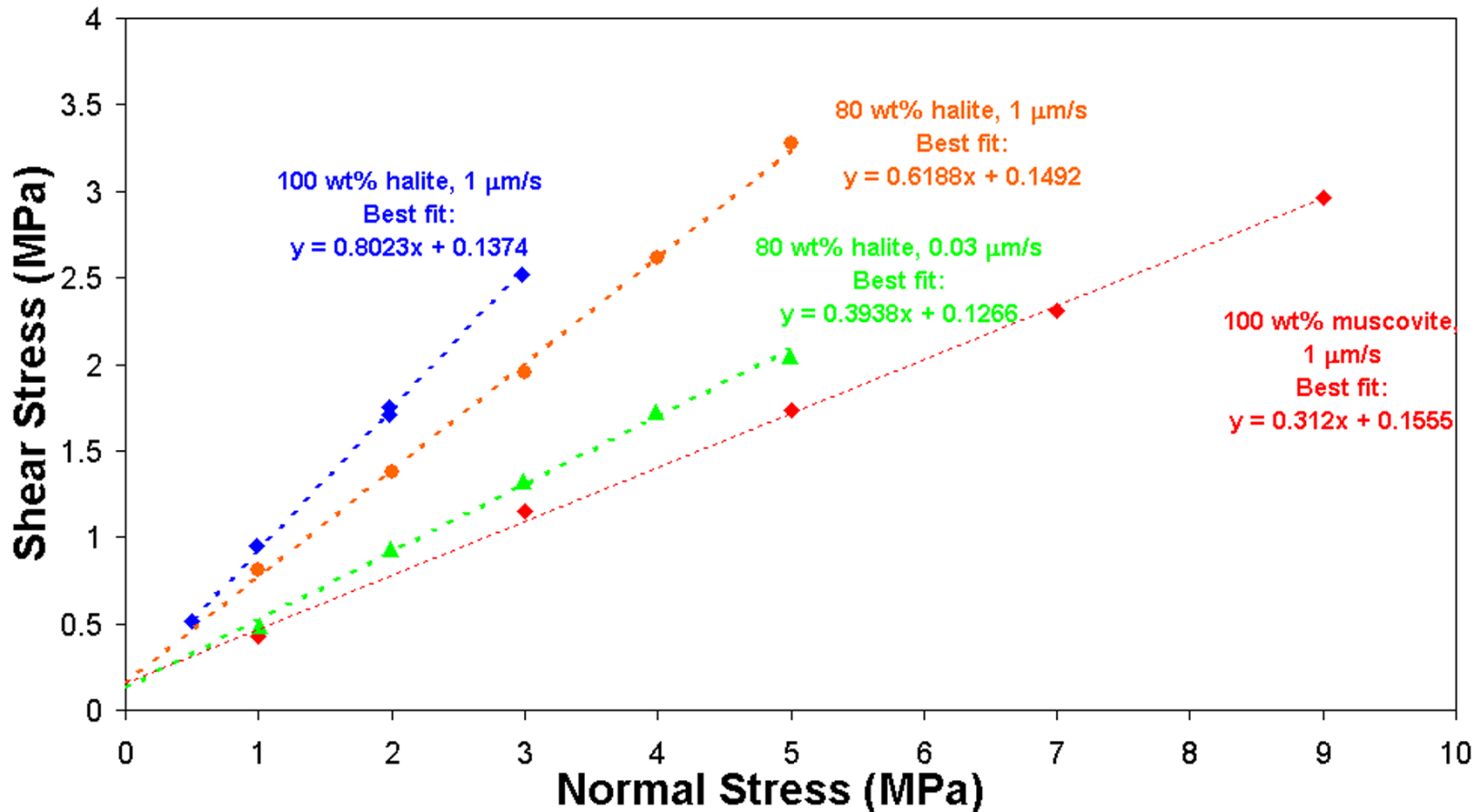
- **Despite > 30 years of work, no microphysical, mechanistic model for friction of fault gouge and its velocity dependence**
- **Extrapolation to natural spatial and temporal scales difficult**
- **Natural fault zones often contain phyllosilicates which typically form some type of foliation**
- **Fluids are ubiquitous in the Earth's crust → fluid-rock interactions must be considered in friction**

Experiments on simulated fault gouges (cf. Bos and coworkers, 2000)

- Granular Halite (grain size $\sim 105 \mu\text{m}$)
- Muscovite (grain size $\sim 13 \mu\text{m}$)
- Initial gouge thickness of $\sim 2 \text{ mm}$.
- Saturated brine as pore fluid (drained)
- Room temperature
- Normal stress: 1 - 5 MPa
- Sliding velocity: 0.001 – 13 $\mu\text{m/s}$
- Slide-hold-slide tests
- Shear strain up to 150



Normal stress-stepping

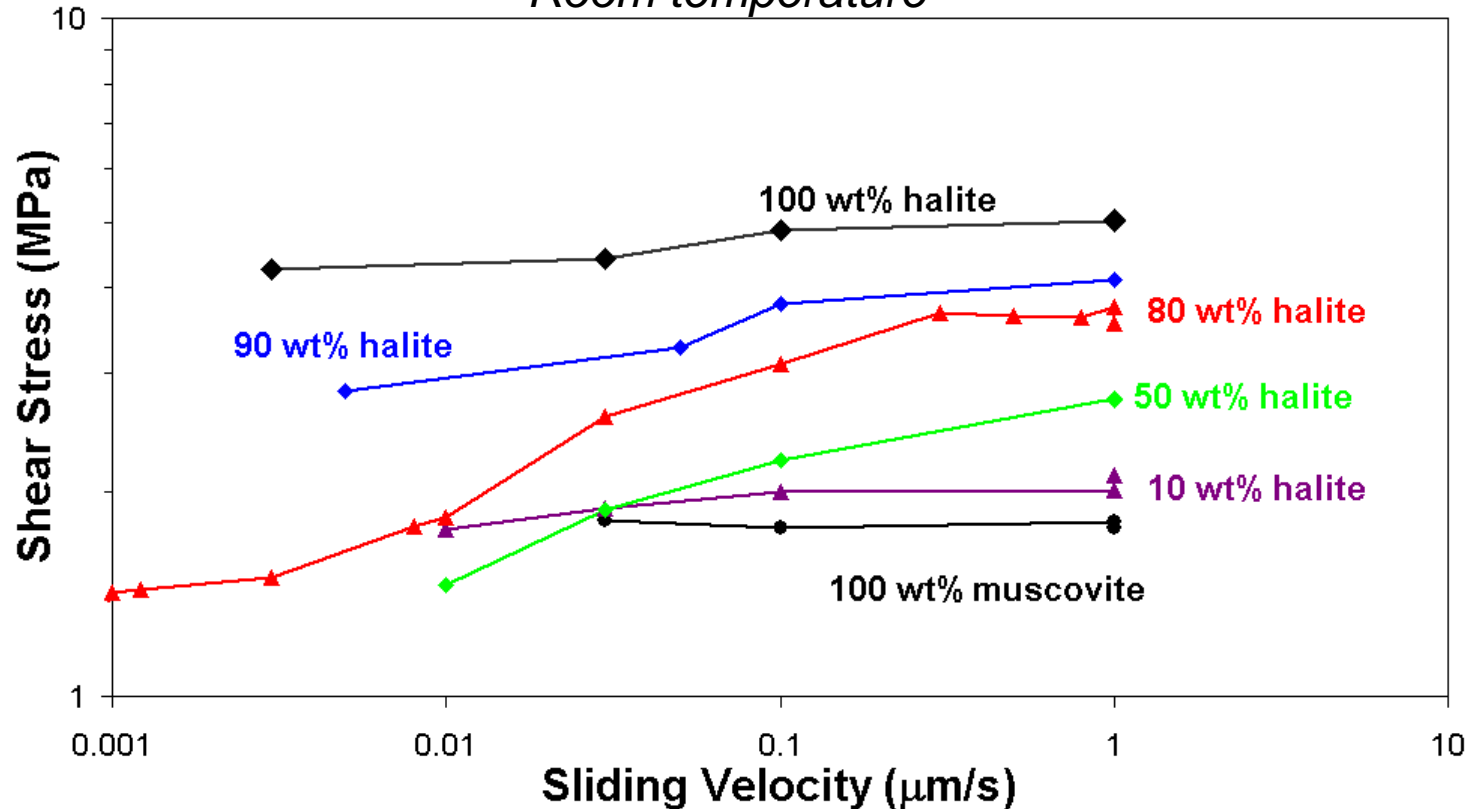


- Linear normal stress dependence – frictional
- Strong dependence of slope on sliding velocity for mixtures

Velocity summary

Normal stress is 5 MPa

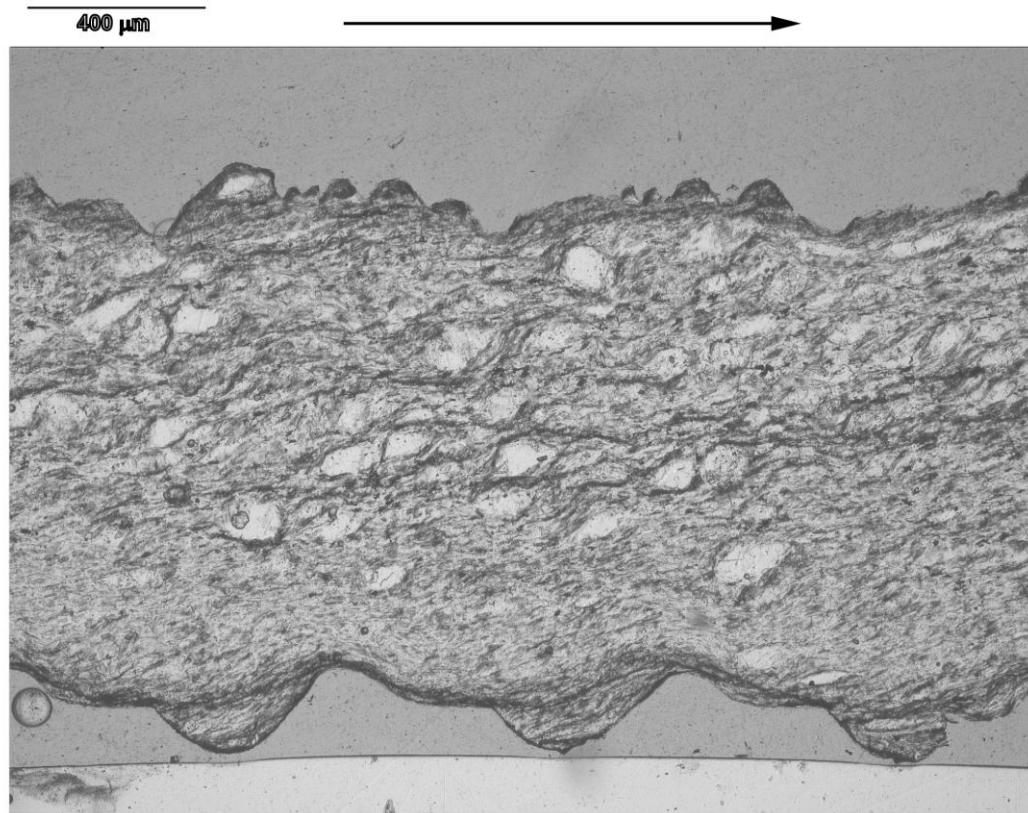
Room temperature



- Friction increases from ~ 0.25 to ~ 0.85 with 3 orders of magnitude change in v for the 80/20 wt% halite/muscovite mixtures
- Average ($a-b$) of almost 0.1
- An order of magnitude larger than “typical” experiments (without fluid-rock interactions)

Microstructures

80 wt% Halite, 20 wt% muscovite 0.03 $\mu\text{m/s}$, 30 mm displacement
Normal stress is 5 MPa



Niemeijer & Spiers,
Geol. Soc, 2005

- Wavy foliation
- Evidence for operation of solution-transfer
- NOTE: no dislocation creep active !!

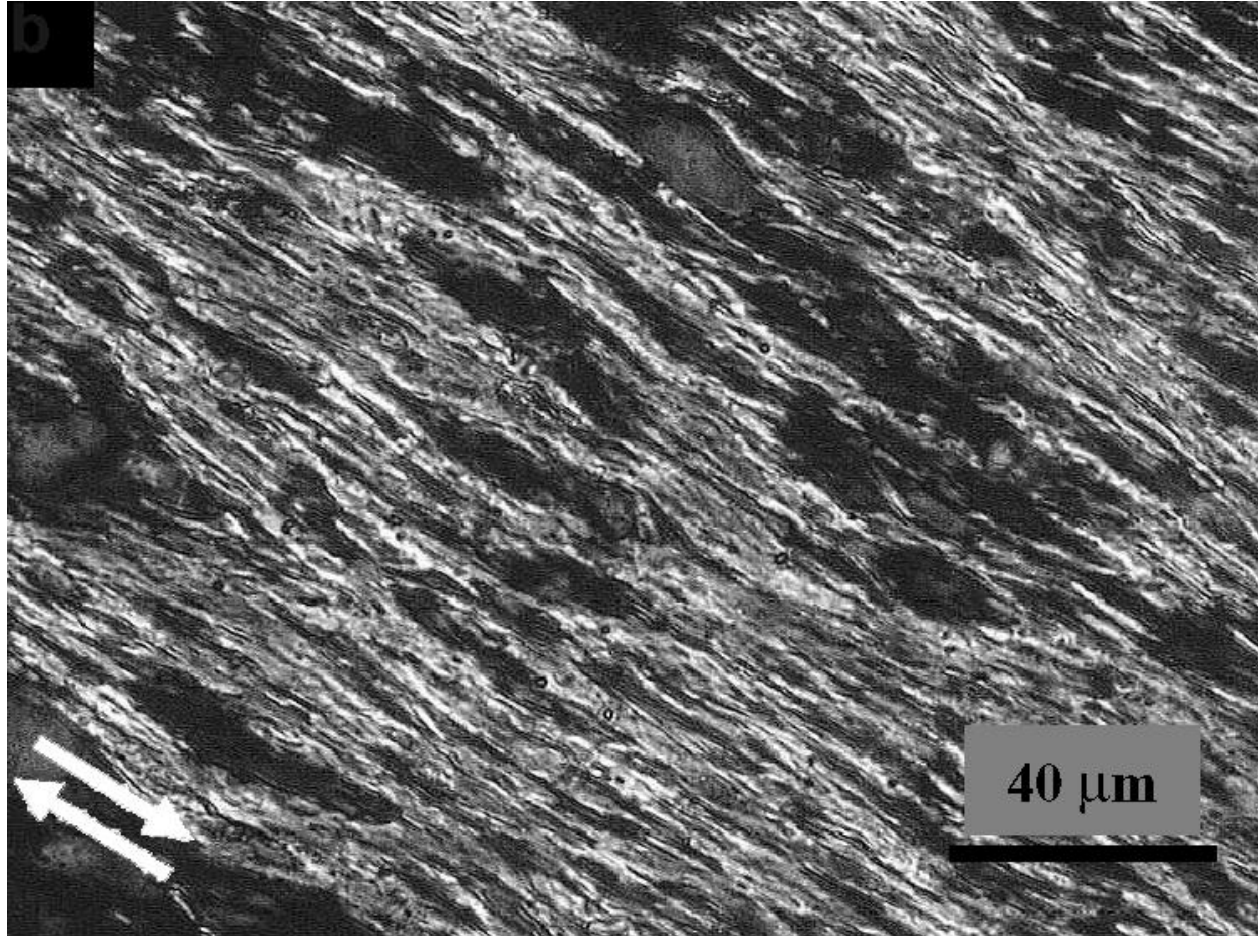
Detail of microstructure

Taken with crossed polarizers



Comparison with natural microstructure

Microstructure from a mica-rich band from a natural shear zone of the Barthelémy massif, French Pyrenees.

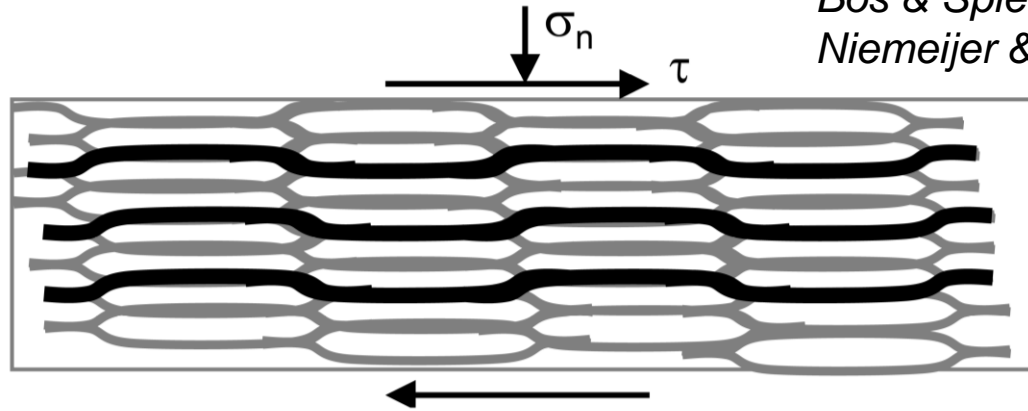


Fine-grained mixture of mica grains (light) and quartz elongated grains (dark).

Deformation mechanism for low velocity regime

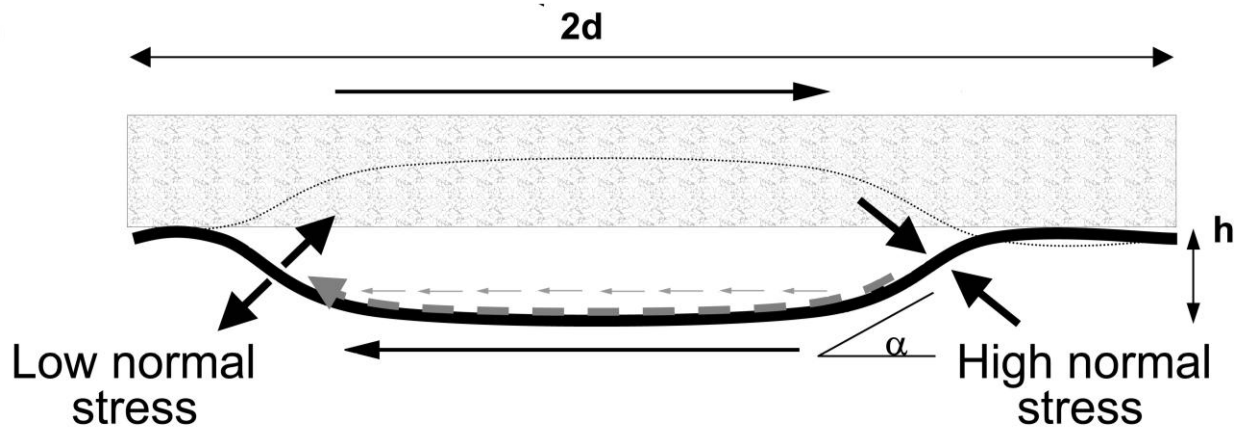
Foliation development followed by frictional sliding on the foliation accommodated by dissolution-diffusion-precipitation of intervening halite grains.

a)

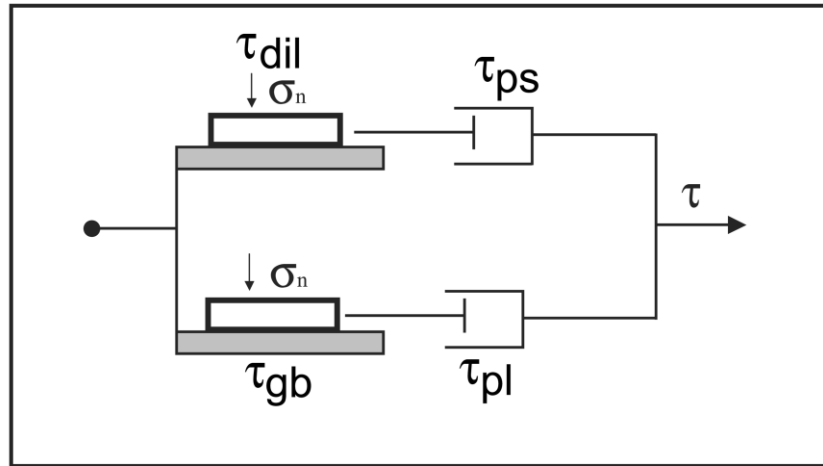


Bos & Spiers, JGR, 2002
Niemeijer & Spiers, Geol. Soc, 2005

b)



Microphysical model



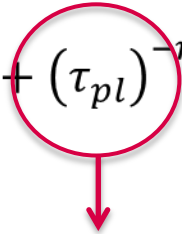
$$\tau = \left\{ (\tau_{gb})^{-m} + (\tau_{pl})^{-m} \right\}^{-\frac{1}{m}} + \left\{ (\tau_{dil})^{-n} + (\tau_{ps})^{-n} \right\}^{-\frac{1}{n}}$$

Shear stress due to sliding over the horizontal part of the wavy foliation

$$\tau_{gb} = P \cdot \mu_{gb} \cdot \sigma_n^{eff}$$

P=factor expressing the proportion of the foliation undergoing active sliding (3/4)

Microphysical model

$$\tau = \left\{ (\tau_{gb})^{-m} + (\tau_{pl})^{-m} \right\}^{-\frac{1}{m}} + \left\{ (\tau_{dil})^{-n} + (\tau_{ps})^{-n} \right\}^{-\frac{1}{n}}$$


Shear stress contribution due to plastic flow of the phyllosilicate foliae

From compressive experiments on e.g. biotite (Kronenberg, et al 1990)

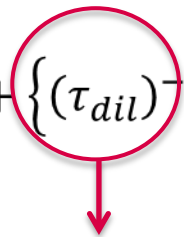
$$\dot{\epsilon} = C \cdot \exp(\alpha \cdot \sigma_d) \exp\left(\frac{-Q}{RT}\right)$$

$\dot{\epsilon}$ axial strain rate, σ_d differential stress, C , α empirical constants, Q apparent activation energy

Rearranging and converting for simple shear due to dislocation slip on (001) gives:

$$\tau_{pl} = \frac{1}{\alpha} \text{Log} \left\{ \frac{3^{\frac{1}{2}} \dot{\gamma}_{pl}}{C \cdot \exp(-Q/RT)} \right\}$$

Microphysical model

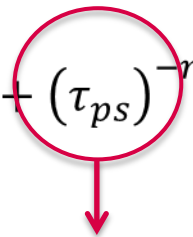
$$\tau = \left\{ (\tau_{gb})^{-m} + (\tau_{pl})^{-m} \right\}^{-\frac{1}{m}} + \left\{ (\tau_{dil})^{-n} + (\tau_{ps})^{-n} \right\}^{-\frac{1}{n}}$$


Shear stress contribution due to work against normal stress to cause dilatation

$$\tau_{dil} = \sigma_n^{eff} \cdot \tan \alpha$$

With α being a geometrical parameter describing the angle of dilatation

Microphysical model

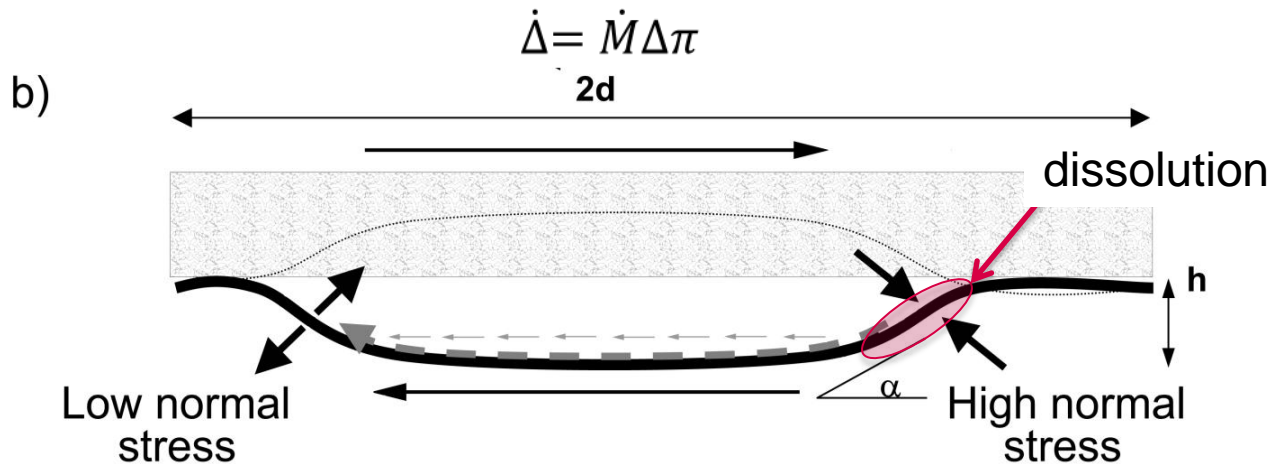
$$\tau = \left\{ (\tau_{gb})^{-m} + (\tau_{pl})^{-m} \right\}^{-\frac{1}{m}} + \left\{ (\tau_{dil})^{-n} + (\tau_{ps})^{-n} \right\}^{-\frac{1}{n}}$$


Shear stress contribution due to pressure solution

- No increase in internal energy/entropy \rightarrow rate of external work equals rate of dissipation (1st law of thermodynamics; isovolumetric deformation)

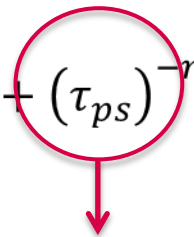
$$\tau \dot{\gamma} = \dot{\Delta}$$

- Rate of dissipation equals mass rate (per unit volume) times the driving force



Rate of pressure solution controlled by the slowest of three serial processes, dissolution, diffusion or precipitation

Microphysical model

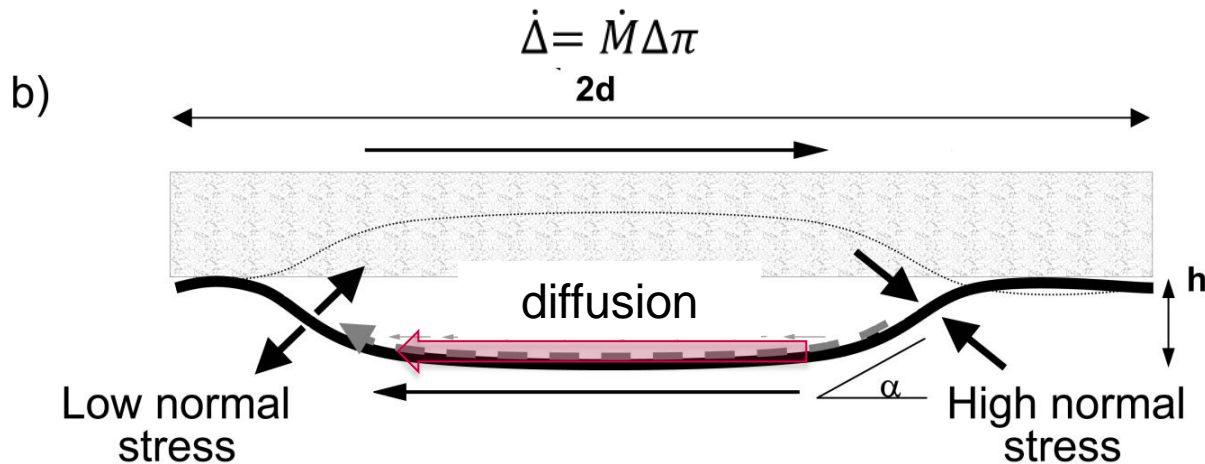
$$\tau = \left\{ (\tau_{gb})^{-m} + (\tau_{pl})^{-m} \right\}^{-\frac{1}{m}} + \left\{ (\tau_{dil})^{-n} + (\tau_{ps})^{-n} \right\}^{-\frac{1}{n}}$$


Shear stress contribution due to pressure solution

- No increase in internal energy/entropy \rightarrow rate of external work equals rate of dissipation (1st law of thermodynamics; isovolumetric deformation)

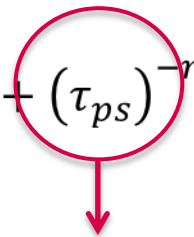
$$\tau \dot{\gamma} = \dot{\Delta}$$

- Rate of dissipation equals mass rate (per unit volume) times the driving force



Rate of pressure solution controlled by the slowest of three serial processes, dissolution, diffusion or precipitation

Microphysical model

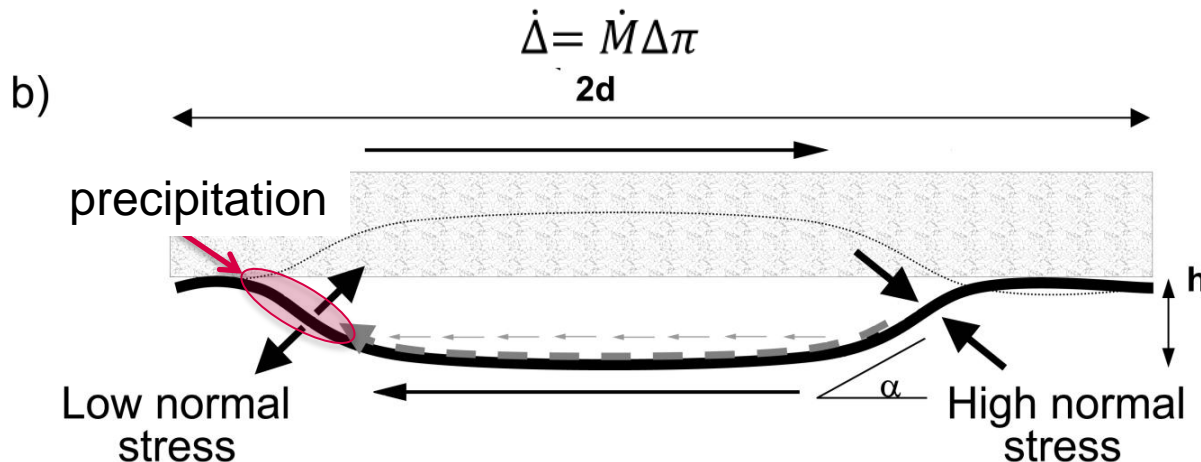
$$\tau = \left\{ (\tau_{gb})^{-m} + (\tau_{pl})^{-m} \right\}^{-\frac{1}{m}} + \left\{ (\tau_{dil})^{-n} + (\tau_{ps})^{-n} \right\}^{-\frac{1}{n}}$$


Shear stress contribution due to pressure solution

- No increase in internal energy/entropy \rightarrow rate of external work equals rate of dissipation (1st law of thermodynamics; isovolumetric deformation)

$$\tau \dot{\gamma} = \dot{\Delta}$$

- Rate of dissipation equals mass rate (per unit volume) times the driving force



Rate of pressure solution controlled by the slowest of three serial processes, dissolution, diffusion or precipitation

Microphysical model

For halite (salt) at these conditions diffusion is the slowest process

- Start with Fick's law for diffusion along the foliation

$$J = P_f D \text{grad} C$$

- For each grain, diffusion works through a window $w\delta$, so flux per grain is
(w grain length out of plane, δ is fluid film thickness)

$$J^* = p_f w \delta D \text{grad} C$$

- Concentration gradient can be expressed as a function of the driving force:

$$\text{grad} C = \frac{C_s M_s}{RT} \text{grad} \pi$$

- Assume the gradient occurs over an average diffusion distance d gives the mass flux

$$\dot{m} = \frac{p_f w \delta D C_s M_s}{RT d} \Delta \pi$$

- Multiply with the number of foliation leading edges actively undergoing pressure solution, $N=A/hwd$ per unit volume gives the macroscopic mass transfer rate:

$$\dot{M} = \frac{A p_f w \delta D C_s M_s}{RT h d^2} \Delta \pi$$

Microphysical model

- Combine equations to get energy dissipation

$$\dot{\Delta} = \dot{M} \Delta\pi \quad \text{and} \quad \dot{M} = \frac{Ap_f w \delta DC_s M_s}{RThd^2} \Delta\pi \quad \Rightarrow \quad \dot{\Delta} = \frac{RThd^2}{Ap_f w \delta DC_s M_s} \dot{M}^2$$

- Derive mass transfer rate geometrically:

$$\dot{\gamma} = \frac{Av_{diss}}{h}$$

- Assuming the dissolving contact has area $hw/\sin\alpha$, gives the mass transfer rate per grain

$$\dot{m} = hw\rho_s v_{diss}$$

- Using these two equations and the number of actively sliding foliation planes, $N=A/hwd$ per unit volume gives the macroscopic mass transfer rate:


$$\dot{M} = \frac{hp_s}{d} \dot{\gamma}$$

- And the dissipation rate:

$$\dot{\Delta} = \frac{RTh^3 \rho_s^2}{Ap_f w \delta DC_s M_s} \dot{\gamma}^2$$

Microphysical model

- Simplify using $\frac{\rho_s}{M_s} = \frac{1}{\Omega_s}$ and $d=B h$, where B is the aspect ratio of the grain

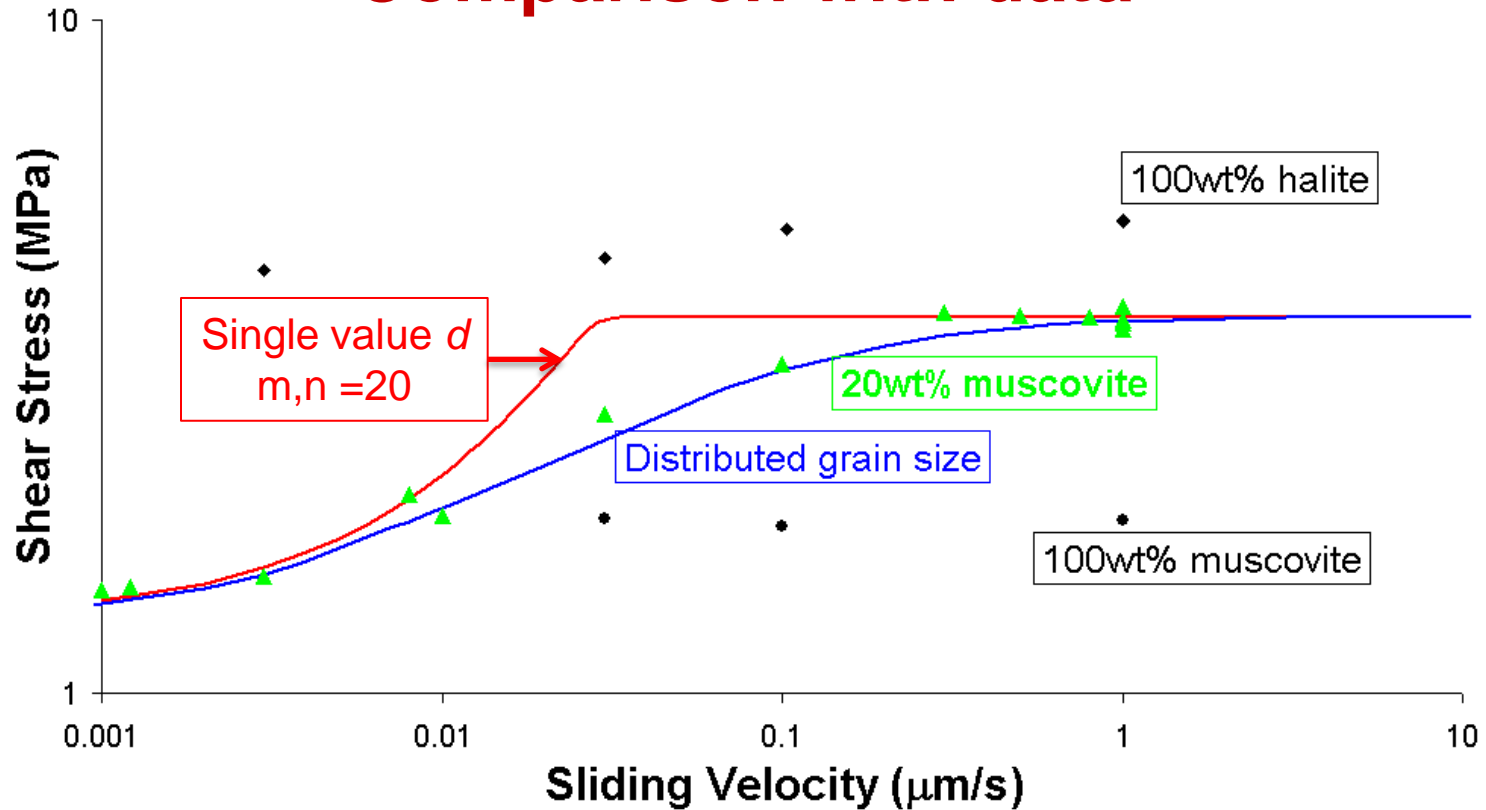

$$\dot{\Delta} = \frac{\alpha \rho_s R T h^3}{\rho_f D \delta C_s \Omega_s} \dot{\gamma}^2$$

- As we have $\tau \dot{\gamma} = \dot{\Delta}$ we get for the shear stress contribution due to diffusion-controlled pressure solution :

$$\tau_{ps} = \frac{RT d^3 \rho_s}{B^3 p_f w \delta D C_s \Omega_s} \dot{\gamma}$$

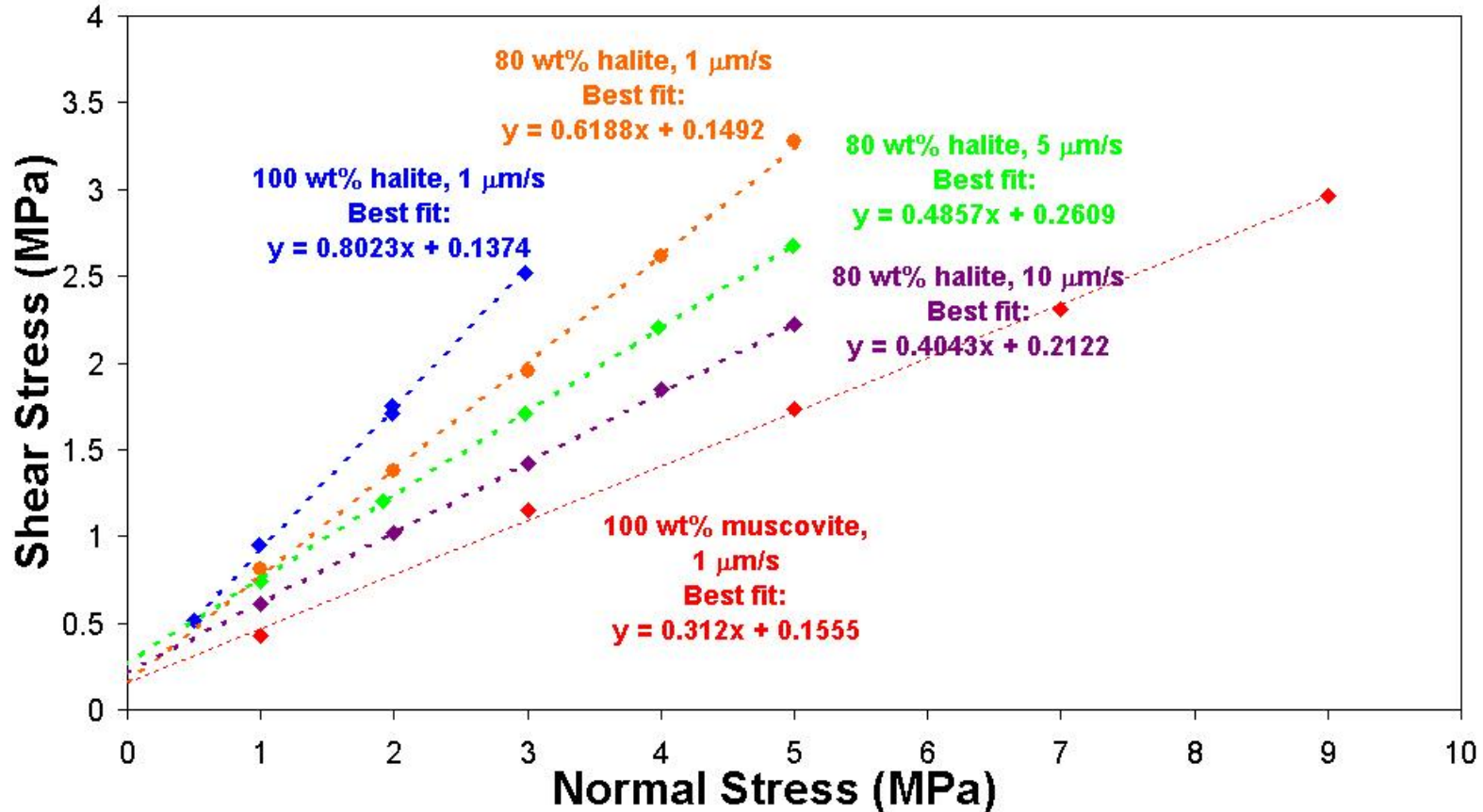
A similar derivation can be done for dissolution and precipitation-controlled pressure solution, see Bos and Spiers, JGR, 2002

Microphysical model Comparison with data



Model reproduces data well, but only if a distributed grain size is used

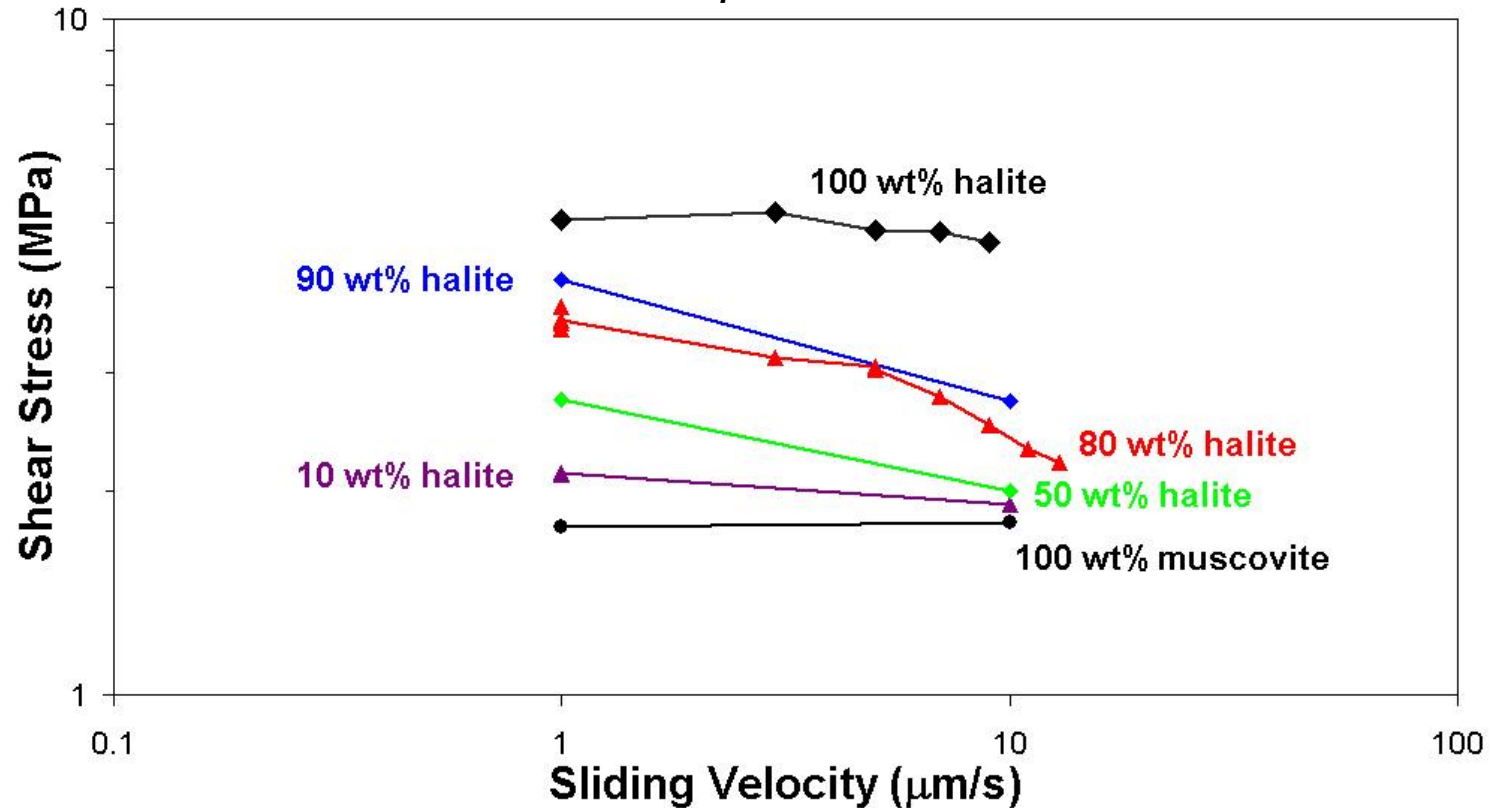
Normal stress-stepping – high(er) velocity



- Linear normal stress dependence – frictional
- Strong dependence of slope on sliding velocity for mixtures

Velocity summary

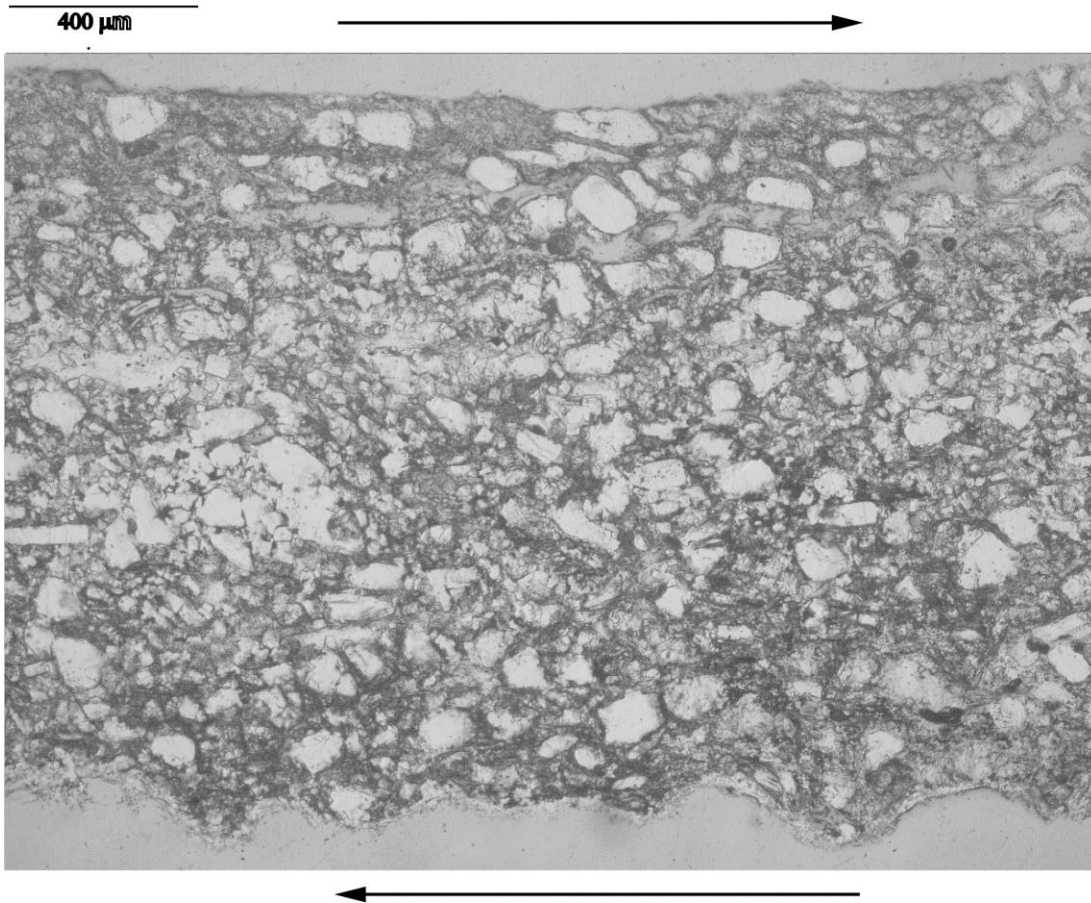
Normal stress is 5 MPa
Room temperature



- Friction decreases from ~ 0.85 to ~ 0.4 within 1.5 orders of magnitude change in v for a 80/20 salt/muscovite mixture
- Average $(a-b)$ of ~ -0.1
- An order of magnitude larger than “typical” experiments (without fluid-rock interactions)

Microstructures

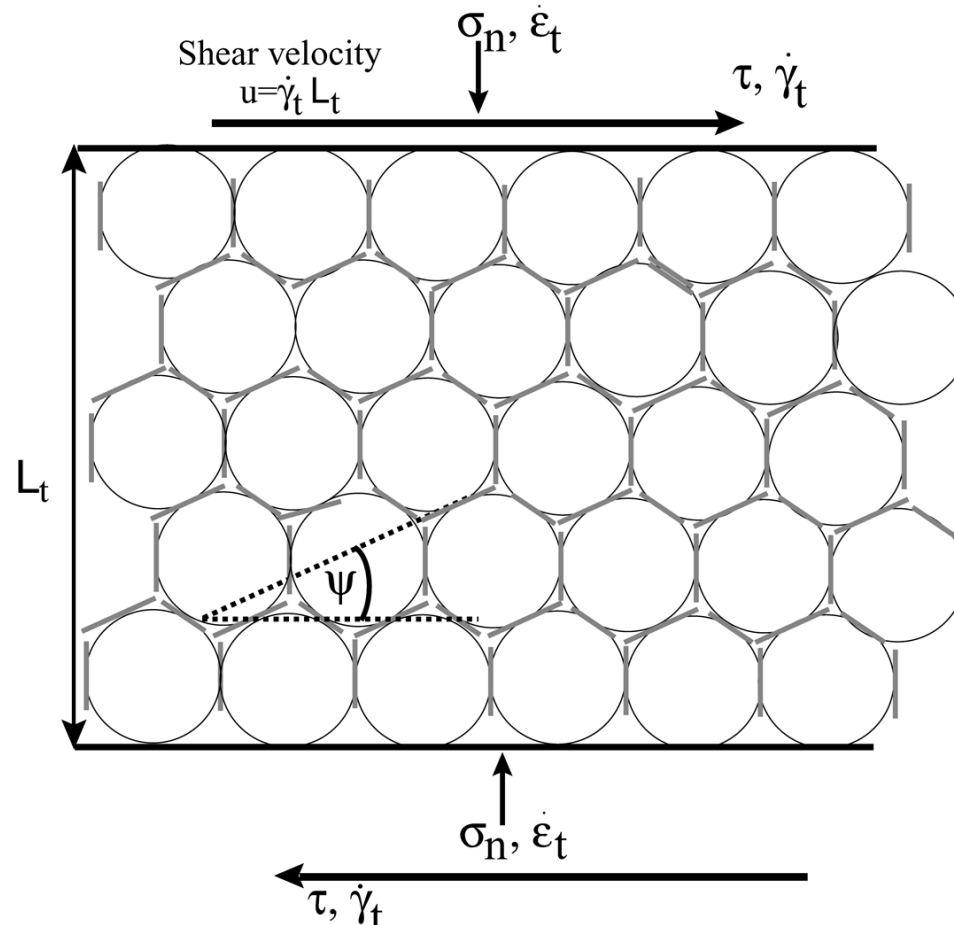
80 wt% halite, 20 wt% muscovite 13 $\mu\text{m/s}$, 30 mm displacement
Normal stress is 5 MPa



- No foliation
- Chaotic, structureless
- Dilatation vs. compaction
- Cataclastic flow

Inferred deformation mechanism at high sliding velocity

Granular flow at a critical porosity, controlled by a competition between slip-dependent dilatation and time-dependent compaction



*Niemeijer & Spiers,
JGR, 2007*

Microphysical model

Time-dependent compaction occurs through IPS

See e.g. Niemeijer et al., *EPSL*, 2002, *Pluymakers & Spiers*, *JGR* 2014

dissolution-controlled:

$$\dot{\varepsilon}_s = A_s \frac{I_s \sigma_e \Omega_s}{d RT} f_s(\phi)$$

diffusion-controlled:

$$\dot{\varepsilon}_d = A_d \frac{(DCS)}{d^3} \frac{\sigma_e \Omega_s}{RT} f_d(\phi)$$

precipitation-controlled:

$$\dot{\varepsilon}_p = A_p \frac{I_p \sigma_e \Omega_s}{d RT} f_p(\phi)$$

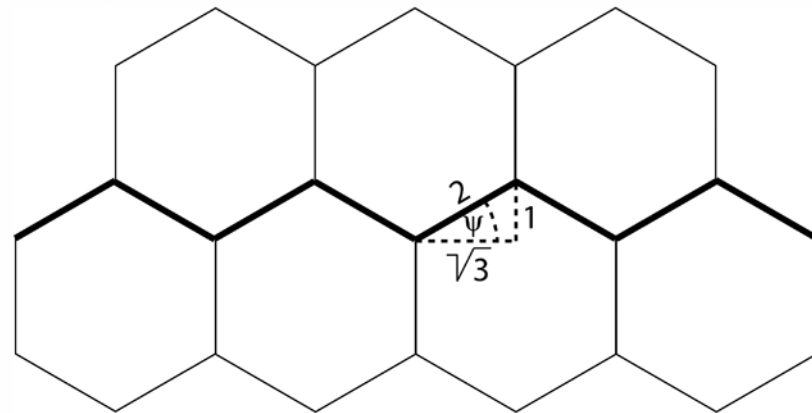
Microphysical model

Dilatancy angle through granular flow

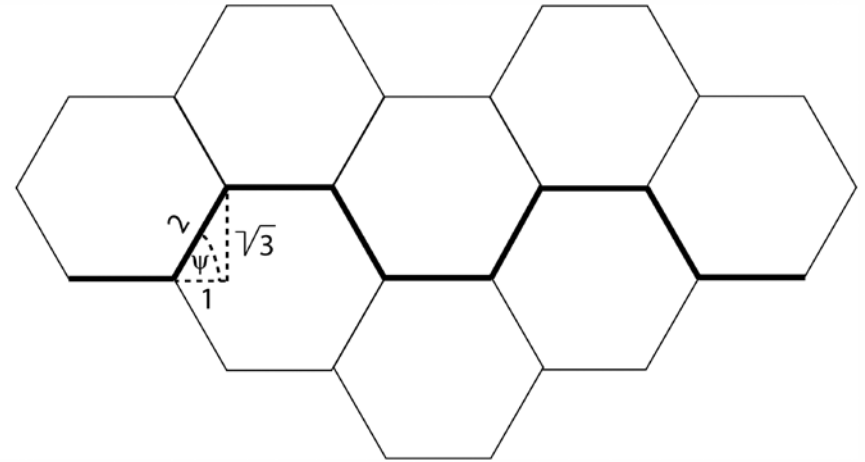
$$\tan\Psi = H(q - 2\phi)^n$$

q takes values of 0.8-1.0

Two possible end members for zero porosity



$$H = \frac{1}{\sqrt{3}}$$



$$H = \sqrt{3}$$

Gives volumetric strain rate due to dilational flow:

$$\dot{\epsilon}_{gr} = -\tan\Psi\dot{\gamma}_t$$

Microphysical model

At steady state, zero volume change:

$$\dot{\epsilon}_{ps} = \dot{\epsilon}_{gr}$$



$$A_s \frac{I_s \sigma_e \Omega_s}{d RT} \frac{1}{(1 - 2\phi)} = -H(q - 2\phi)^n \cdot \dot{\gamma}_t$$

dissolution-control



$$\phi_{ss} \approx \frac{1}{2} \left\{ q - \left(A_s \cdot \frac{I_s}{d} \cdot \frac{\sigma_e \Omega_s}{R \cdot T} \cdot \frac{1}{\dot{\gamma}_t \cdot H} \right)^{\frac{1}{2}} \right\}$$

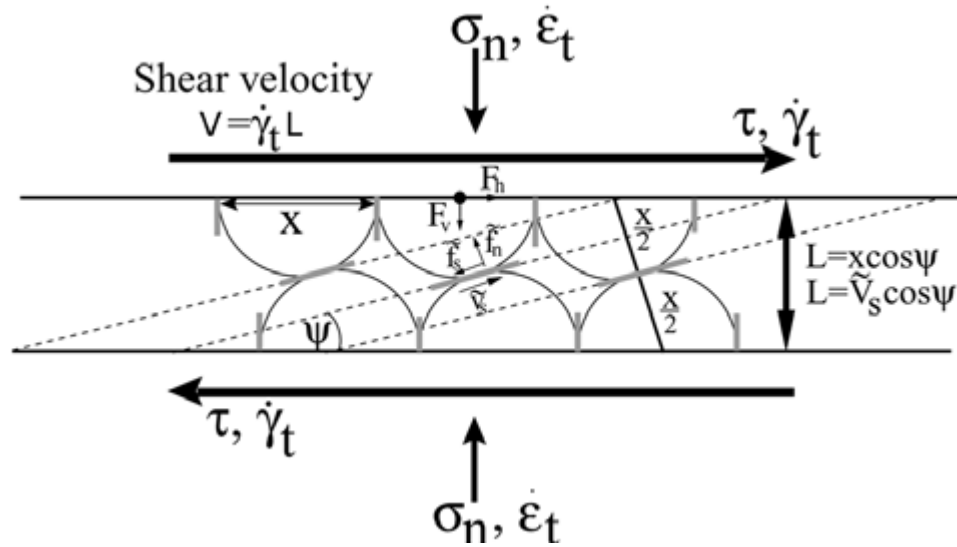
dissolution-control

Or

$$\tan \Psi_{ss} \approx H \left(A_s \cdot \frac{I_s}{d} \cdot \frac{\sigma_e \Omega_s}{R \cdot T} \cdot \frac{1}{\dot{\gamma}_t \cdot H} \right)^{\frac{1}{2}}$$

dissolution-control

Microphysical model



Consider macroscopic forces

horizontal

$$F_h = \tau x^2$$

vertical

$$F_v = \sigma_n x^2$$

Consider contact forces

normal

$$\tilde{f}_n = F_v \cos \Psi + F_h \sin \Psi$$

shear

$$\tilde{f}_s = F_h \cos \Psi - F_v \sin \Psi$$

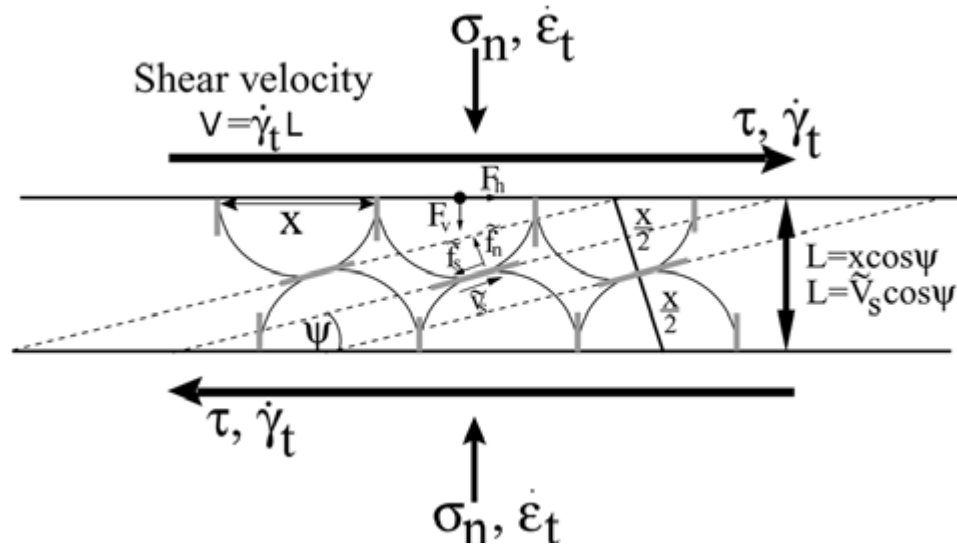


$$\tilde{f}_n = \sigma_n x^2 \cos \Psi + \tau x^2 \sin \Psi$$



$$\tilde{f}_s = \tau x^2 \cos \Psi - \sigma_n x^2 \sin \Psi$$

Microphysical model



Contact area in a compacting aggregate can be approximated by:

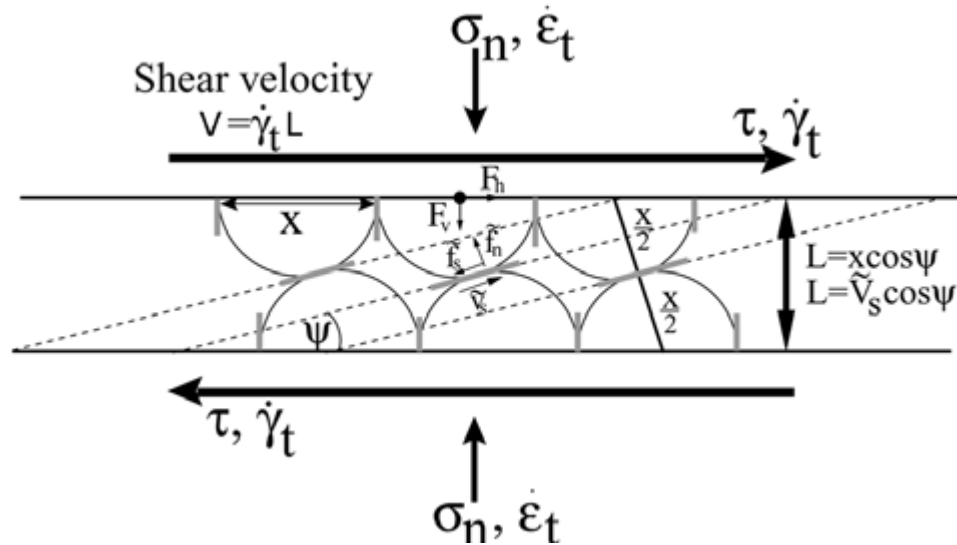
$$A_c = k\pi d^2(q - 2\phi)$$

where $k = 1/6$ (1/grain coordination nr.) and $q \approx 0.8-1.0$

$$\tilde{\sigma}_n = \frac{\tilde{f}_n}{A_c} = \frac{\tilde{f}_n}{k\pi d^2(q - 2\phi)} \quad \text{with } x \approx d \quad \Rightarrow \quad \tilde{\sigma}_n = \frac{1}{k\pi(q - 2\phi)} (\sigma_n \cos \Psi + \tau \sin \Psi)$$

$$\tilde{\tau} = \frac{\tilde{f}_s}{A_c} = \frac{\tilde{f}_s}{k\pi d^2(q - 2\phi)} \quad \text{with } x \approx d \quad \Rightarrow \quad \tilde{\tau} = \frac{1}{k\pi(q - 2\phi)} (\tau \cos \Psi - \sigma_n \sin \Psi)$$

Microphysical model



Contacts obey Coulomb-type slip criterion:

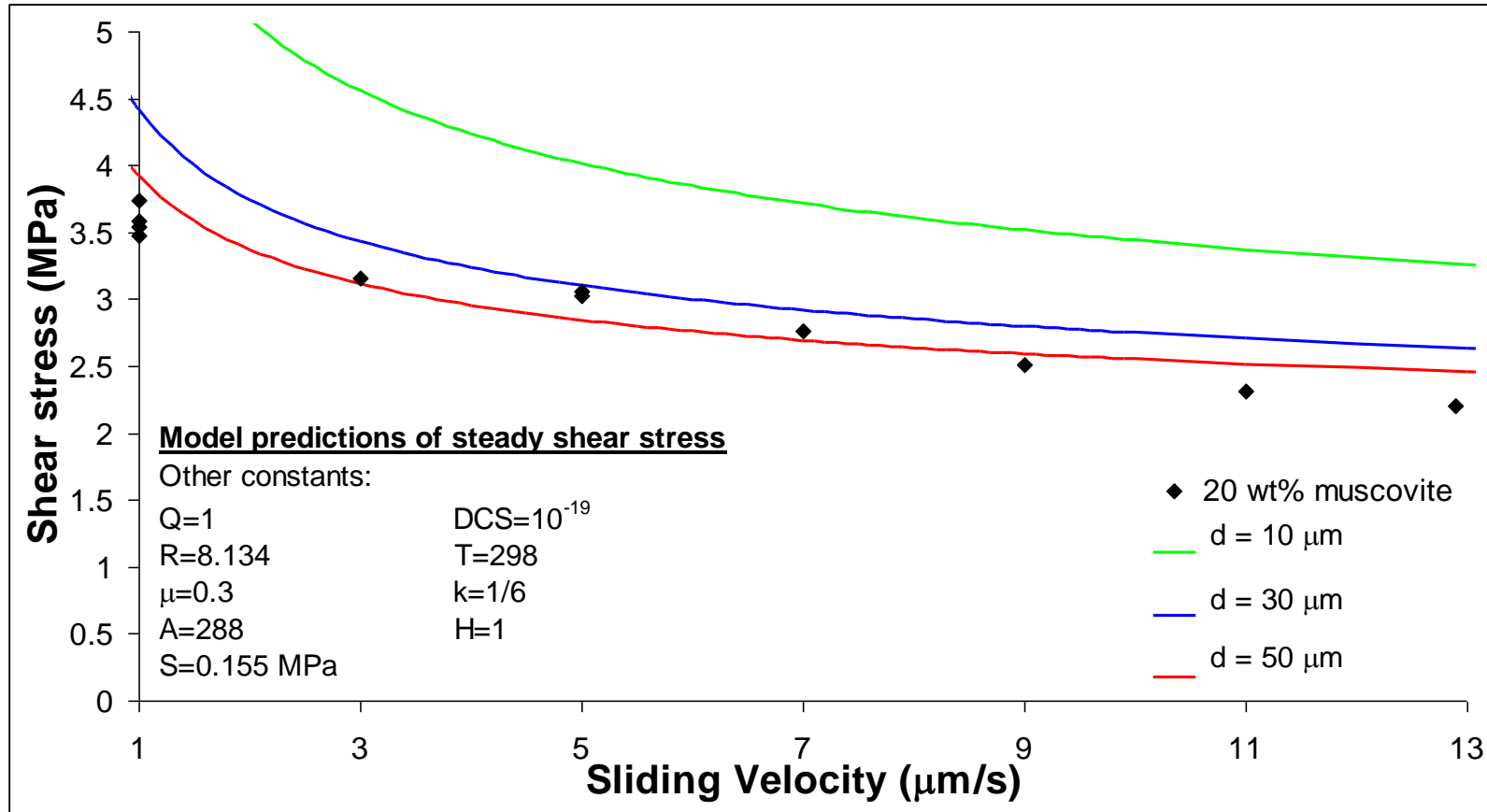
$$\tilde{\tau} = \tilde{S}_0 + \tilde{\mu} \tilde{\sigma}_n$$

where \tilde{S}_0 is the cohesion of the contact

$$\frac{\tau \cos \Psi - \sigma_n \sin \Psi}{k\pi (q - 2\phi)} = \tilde{S}_0 + \tilde{\mu} \frac{\sigma_n \cos \Psi + \tau \sin \Psi}{k\pi (q - 2\phi)}$$

Recall $\tan \Psi = H(q - 2\phi)$ \longrightarrow
$$\tau = \frac{k\pi}{H} \left(\frac{\tan \Psi}{\cos \Psi - \tilde{\mu} \sin \Psi} \right) \tilde{S}_0 + \frac{(\sin \Psi + \tilde{\mu} \cos \Psi)}{(\cos \Psi - \tilde{\mu} \sin \Psi)} \sigma_n$$

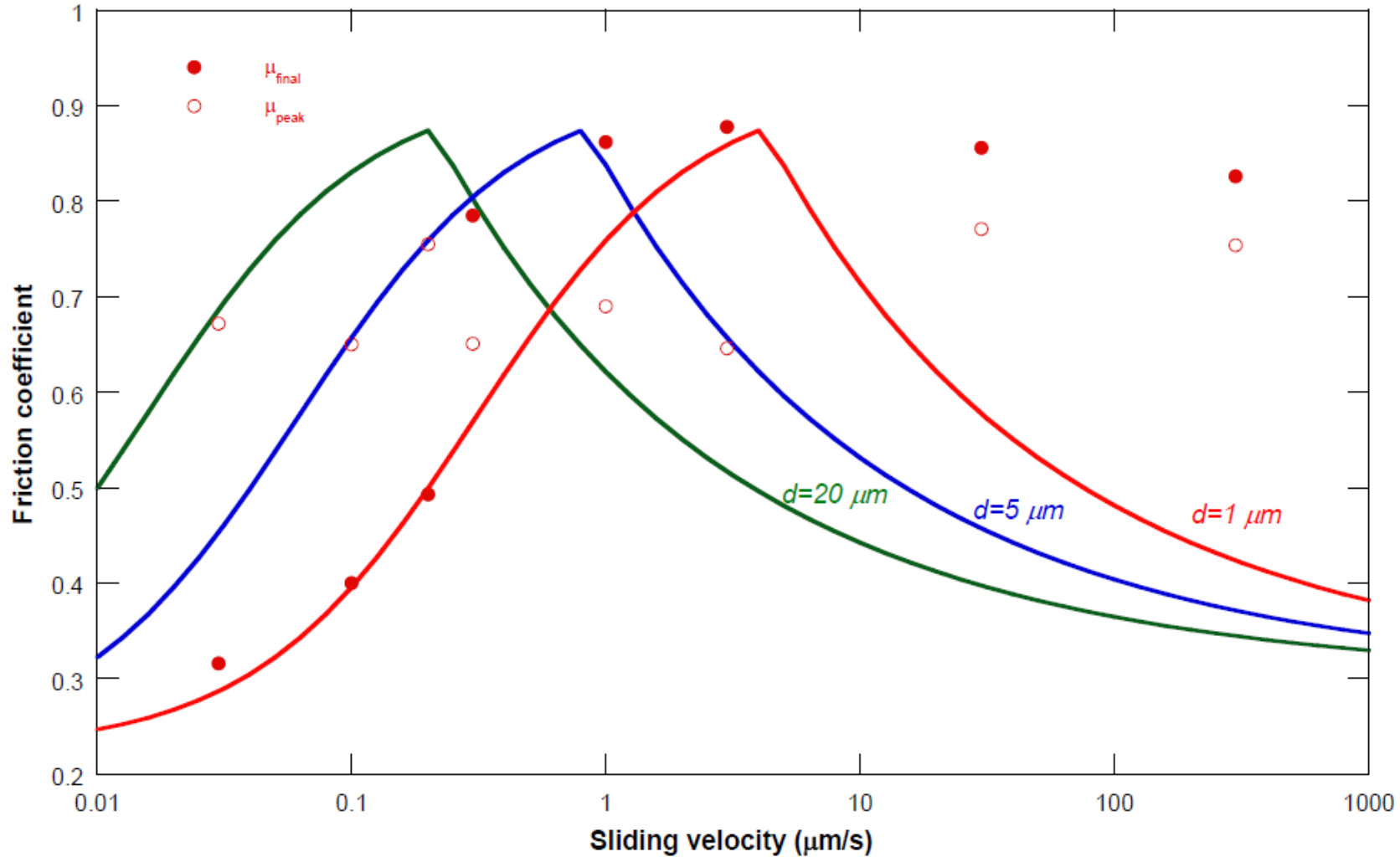
Comparison with experiments



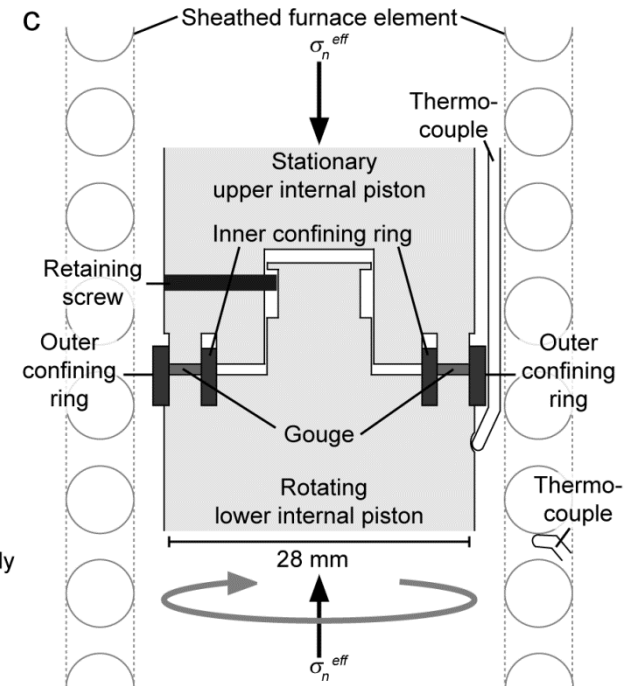
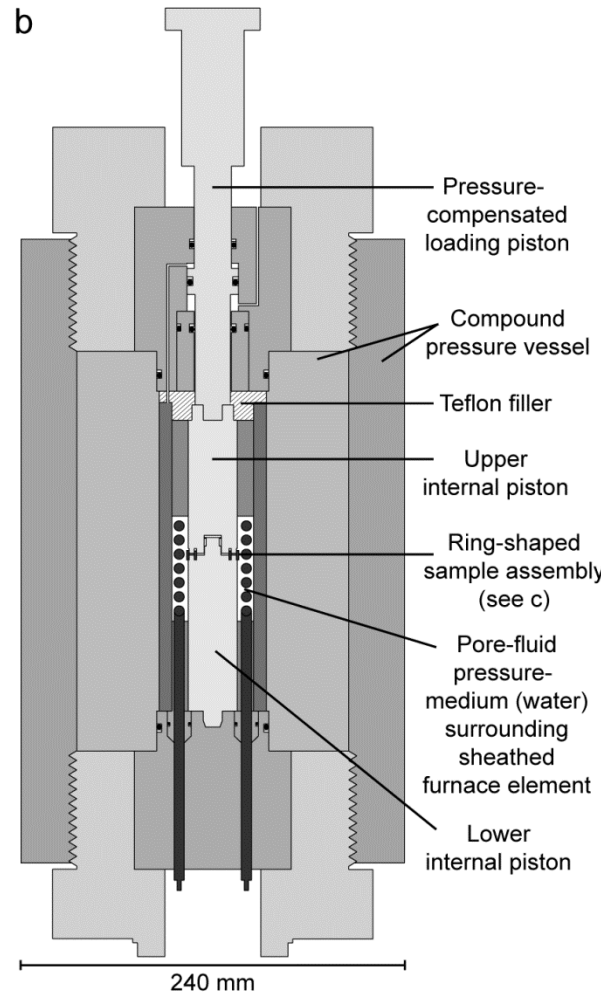
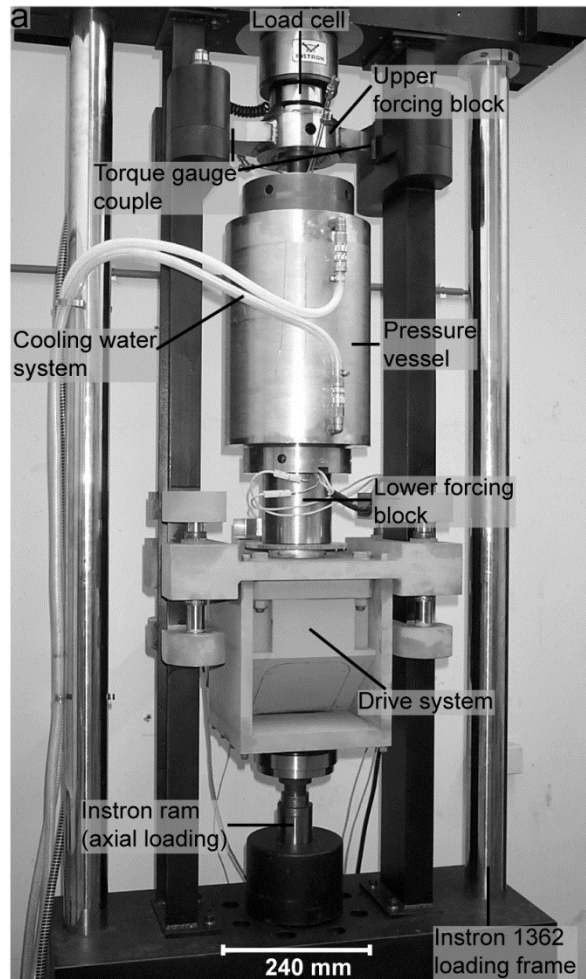
- Effect of grain size on model predictions quite large !
- Likely that grain size varies as a function of sliding velocity

Activation of same mechanisms in real materials:

Recent results from quartz/muscovite experiments
at 500 °C, σ_n^{eff} 120 MPa, Pf 80 MPa, 30 mm displacement

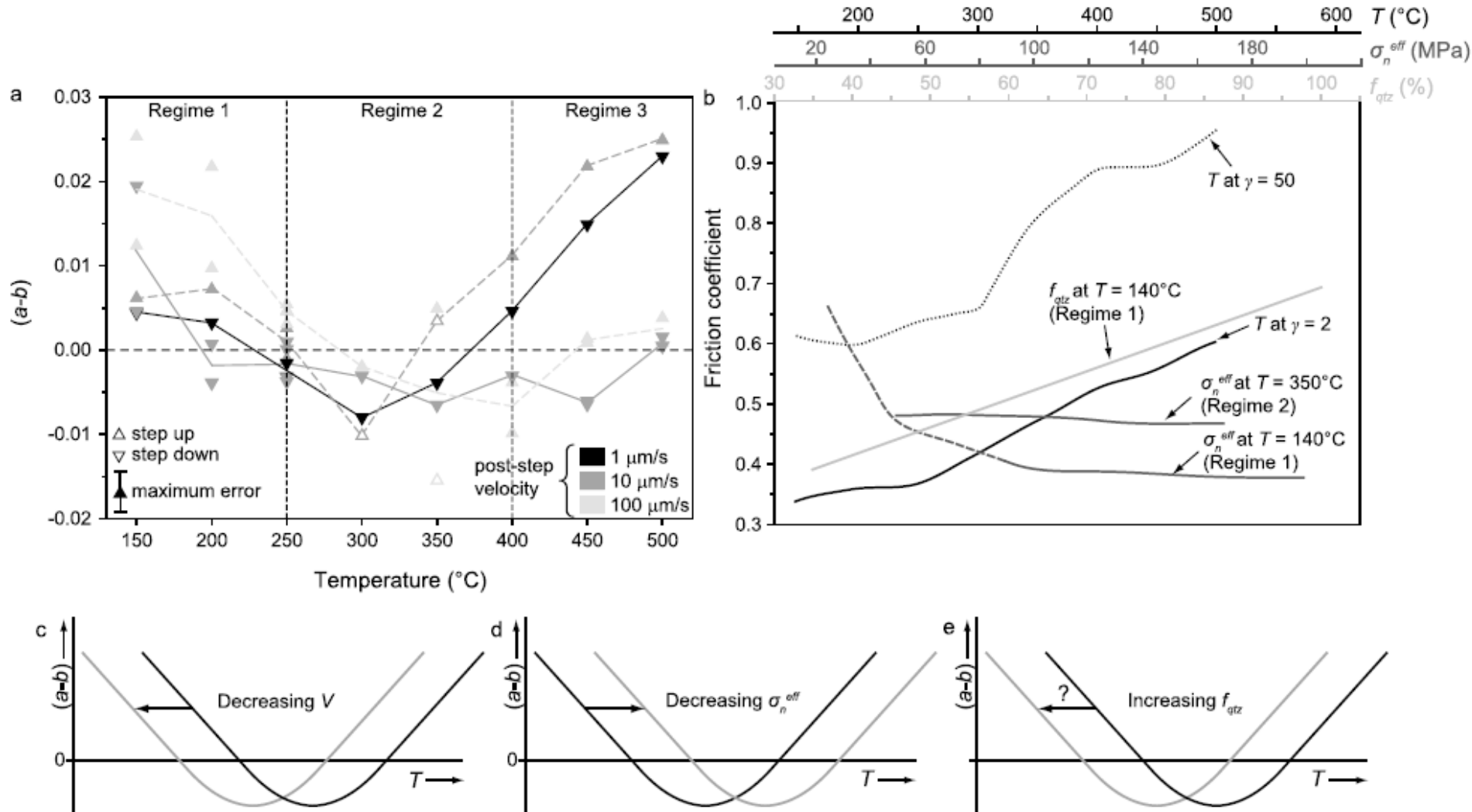


Experiments on simulated megathrust fault gouges at in-situ subduction zone *PT* conditions



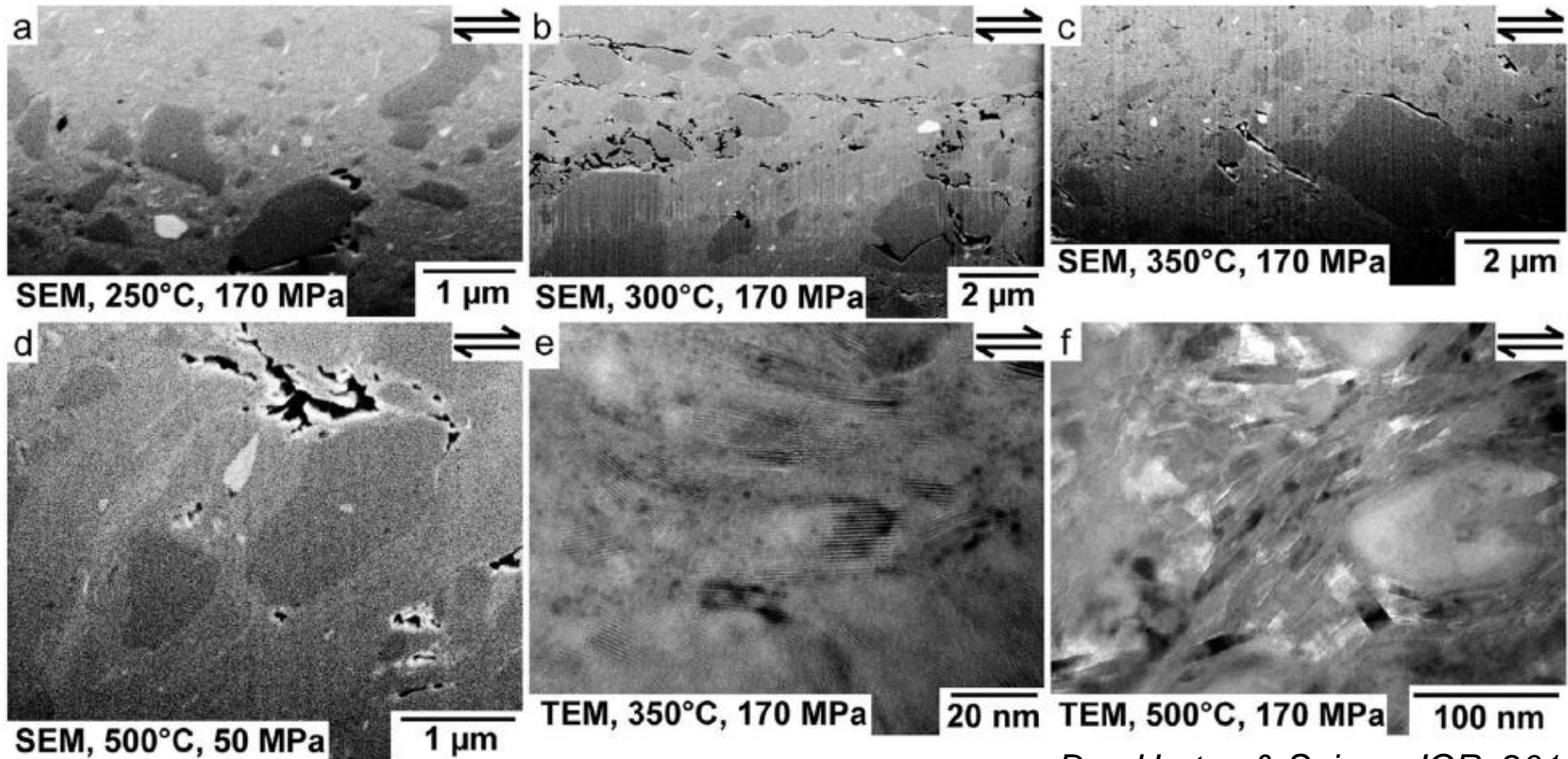
- Illite/qtz gouges (65/35 wt%)
- $T = 150-500^{\circ}\text{C}$
- $\sigma_n^{eff} = 170 \text{ MPa}$
- $P_f = 100 \text{ MPa H}_2\text{O}$
- $V = 1-100 \mu\text{m/s}$
- $\gamma \leq \sim 170$

Main experimental trends



Den Hartog & Spiers, JGR, 2014

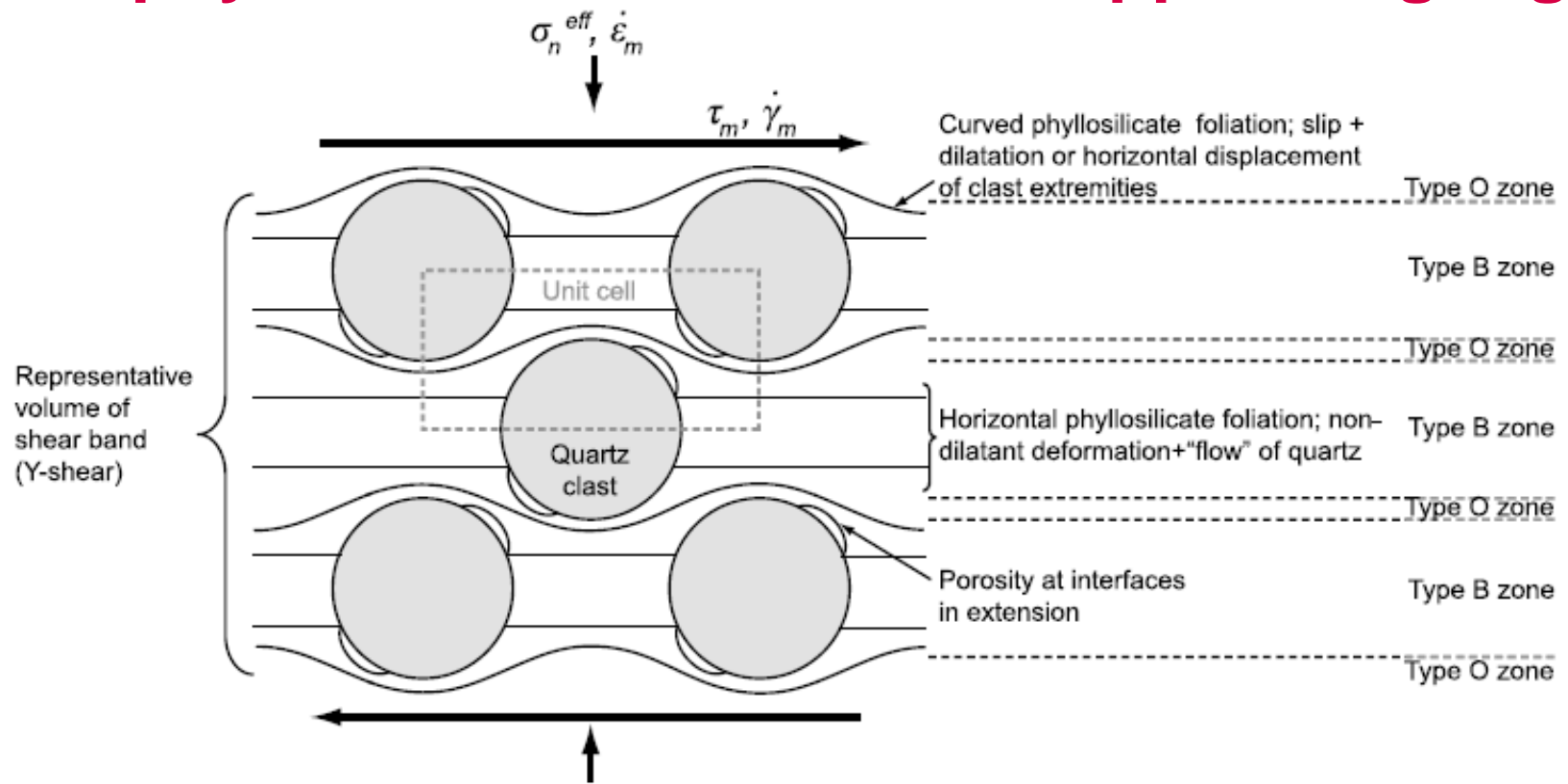
Microstructural observations



Den Hartog & Spiers, JGR, 2014

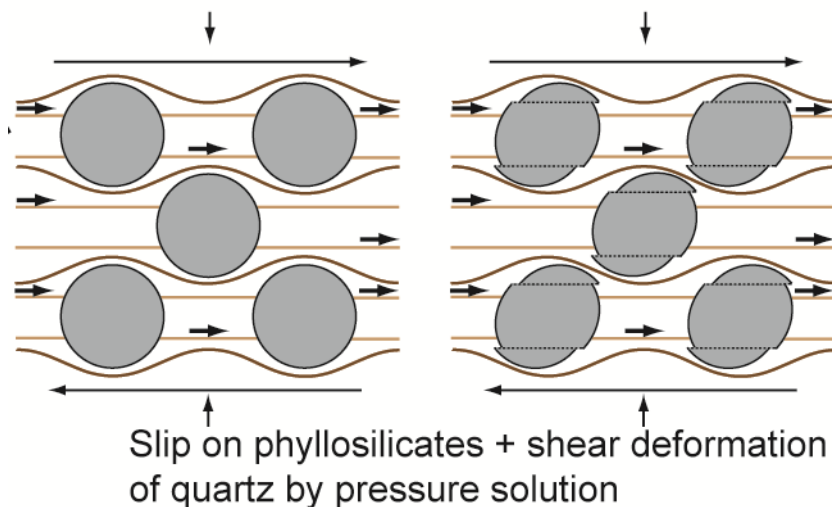
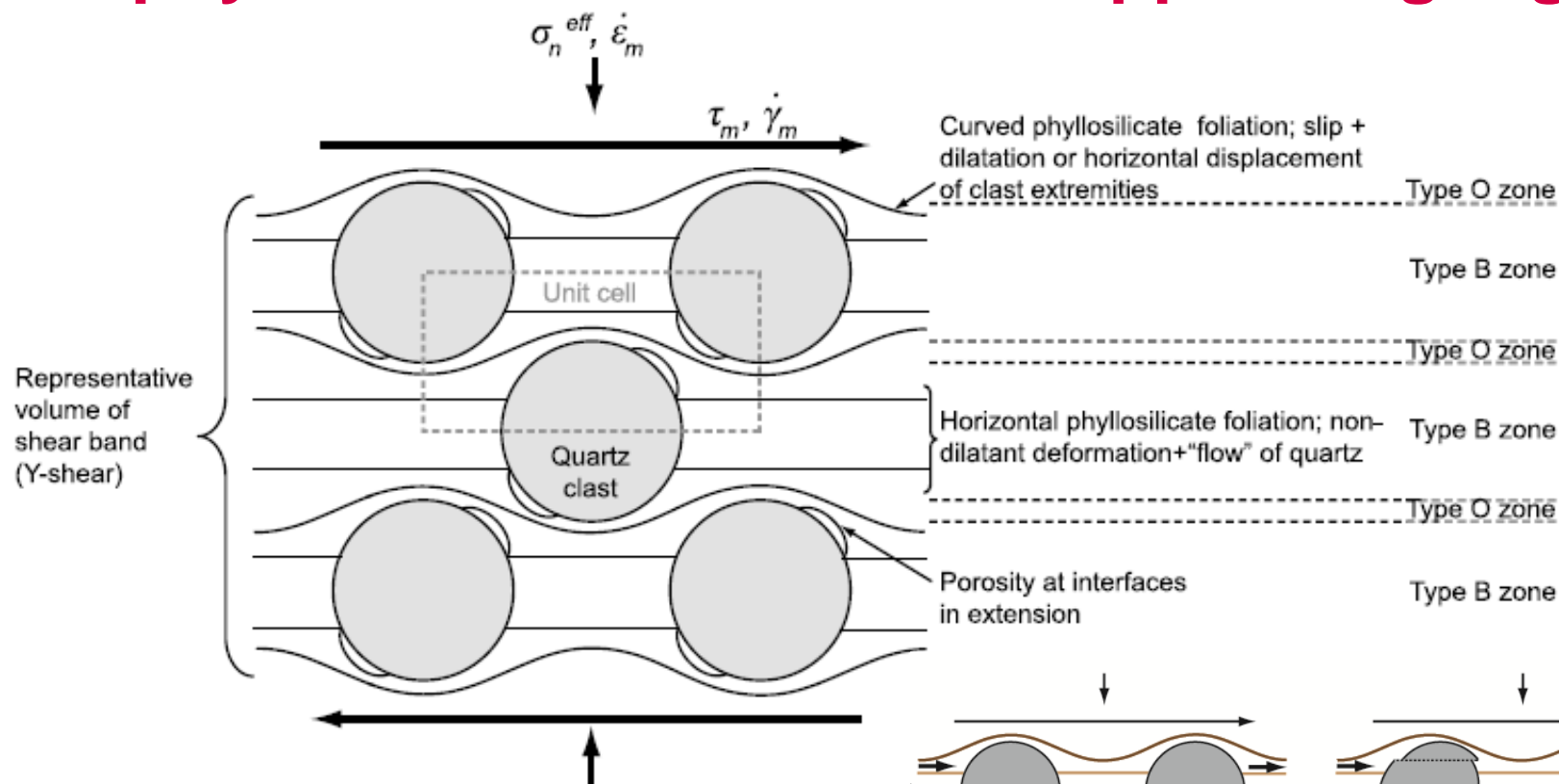
- Phyllosilicate foliation wrapping around quartz clasts.
- Porosity at the clast-phyllosilicate interface under extension.
- Oval quartz shapes \rightarrow pressure solution?
- Matrix supported \rightarrow **cannot be modelled with preceding microphysical models!!**

Microphysical model for matrix-supported gouges



Den Hartog & Spiers, JGR, 2014

Microphysical model for matrix-supported gouges

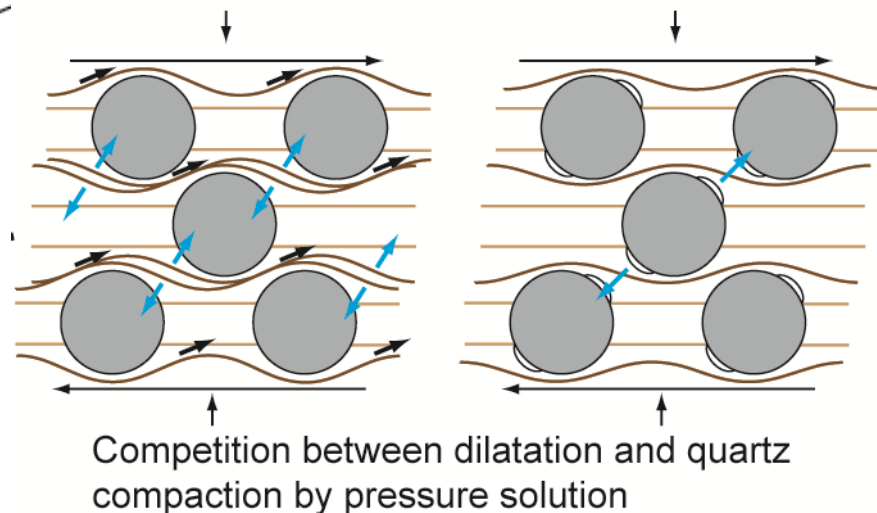
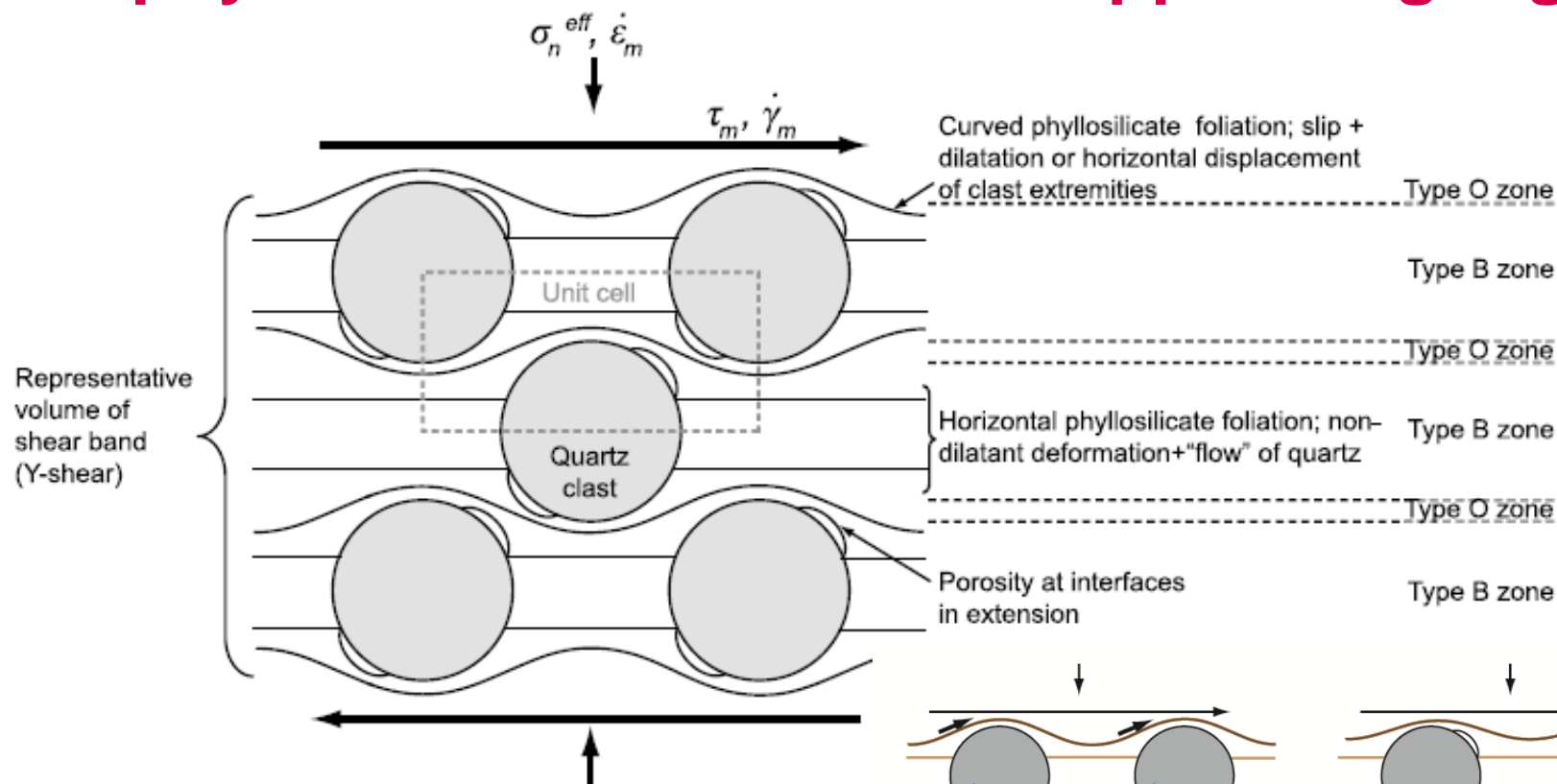


Low V /high T :

- Easy shear deformation of quartz by pressure solution
- Slip on horizontal phyllosilicates with serial shear of quartz "bodies" or "overlaps"

→ **Non-dilatant deformation, $(a-b) > 0$**

Microphysical model for matrix-supported gouges

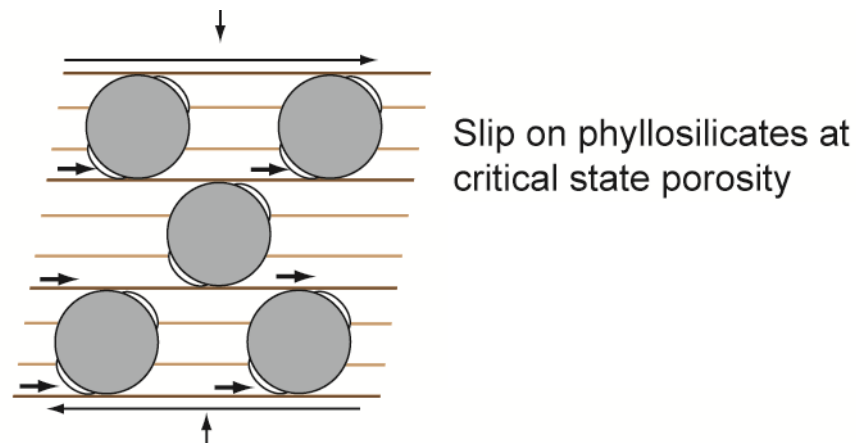
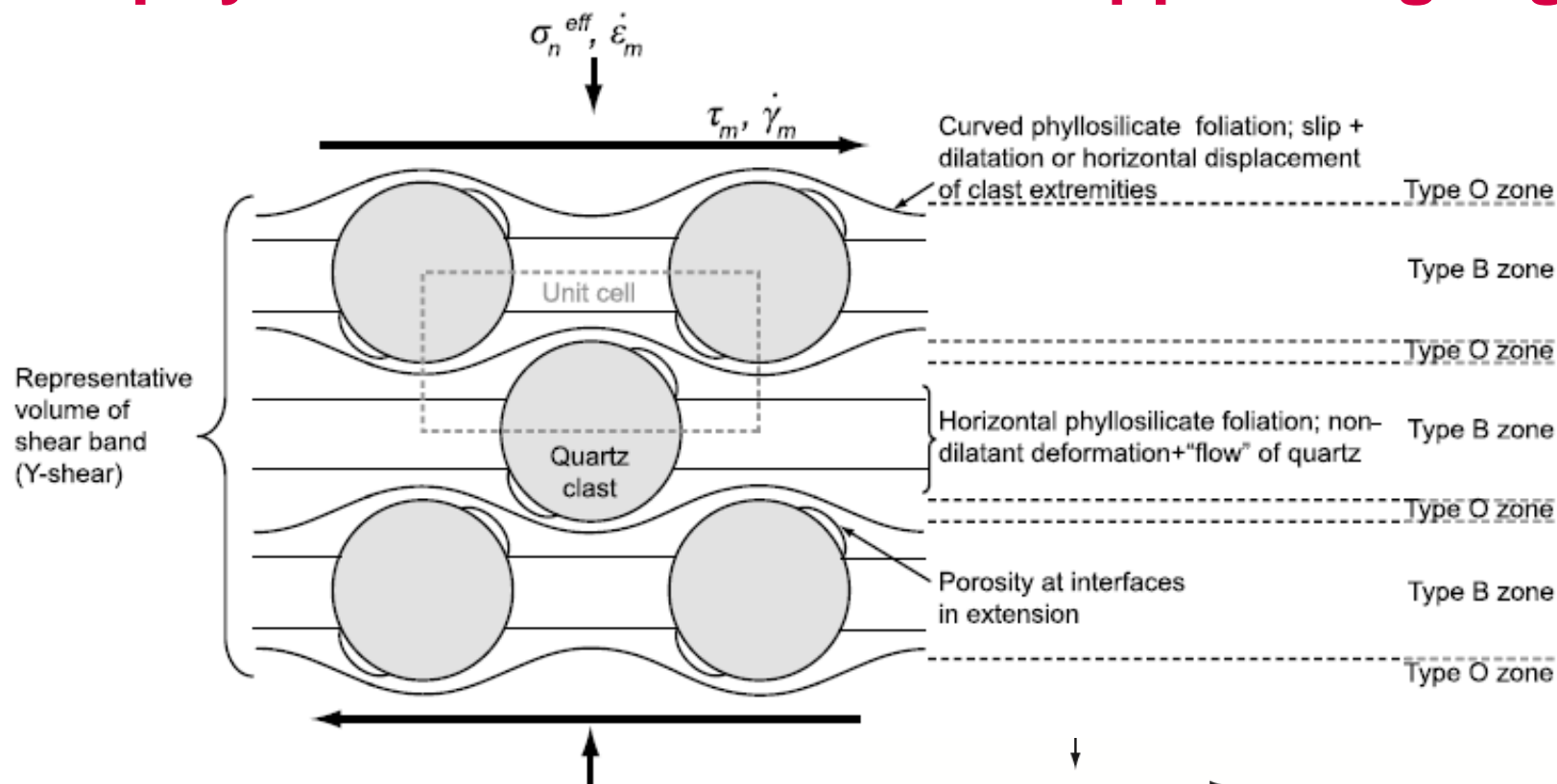


High V /low T :

- Too slow shear deformation of quartz by pressure solution
- Dilatant slip on curved phyllosilicates balanced by compaction of qtz by p.soln.

→ Dilatant deformation, $(a-b) < 0$

Microphysical model for matrix-supported gouges

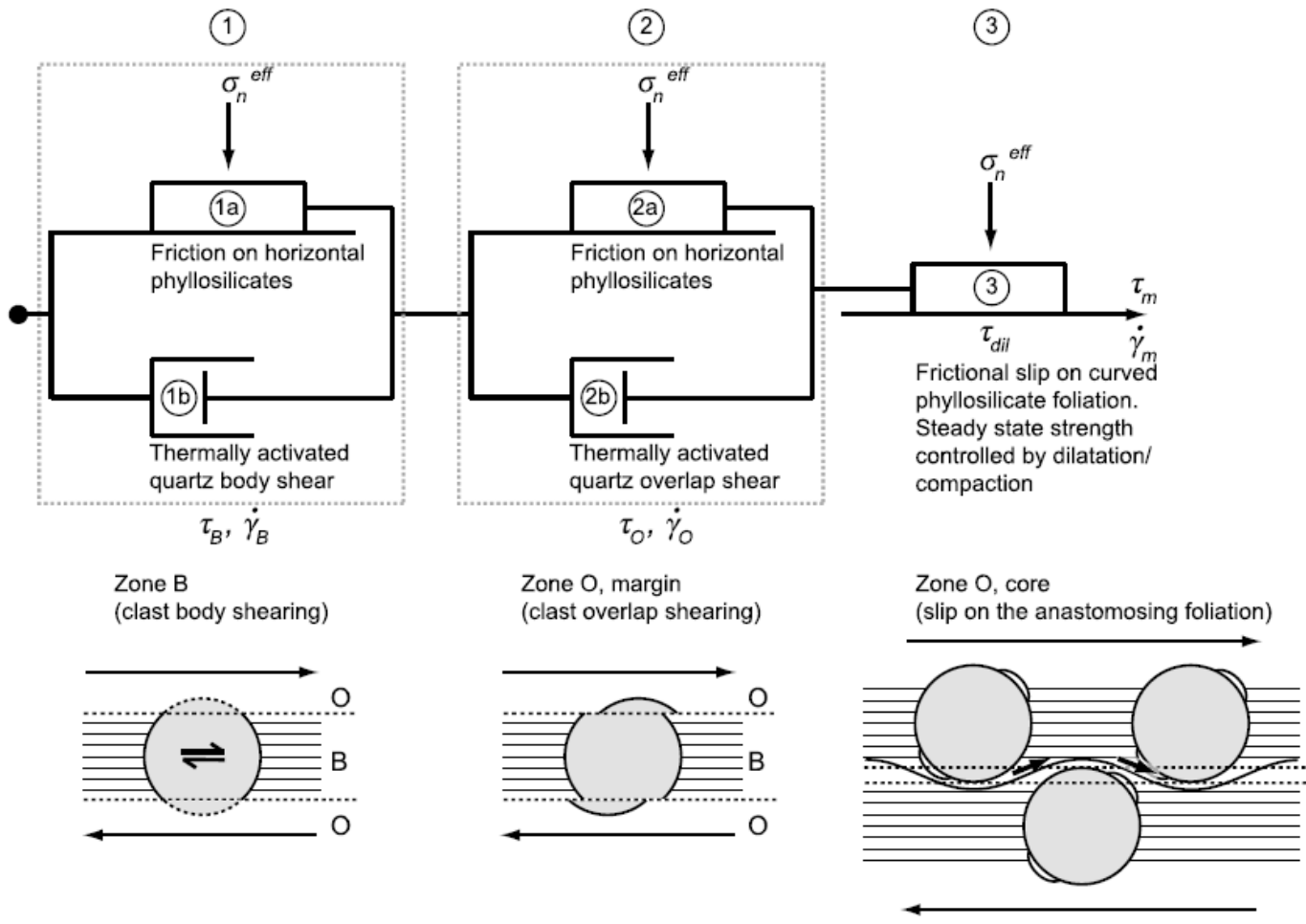


High V /low T :

- Too slow shear deformation of quartz by pressure solution
- Dilatant slip on curved phyllosilicates balanced by compaction of qtz by p.soln.

→ Dilatant deformation, $(a-b) < 0$

Microphysical model for matrix-supported gouges



Non-dilatant deformation:
(1) and (2) active

$$\tau_m = \tau_B = \tau_O$$

$$\dot{\gamma}_m = \dot{\gamma}_B + \dot{\gamma}_O$$

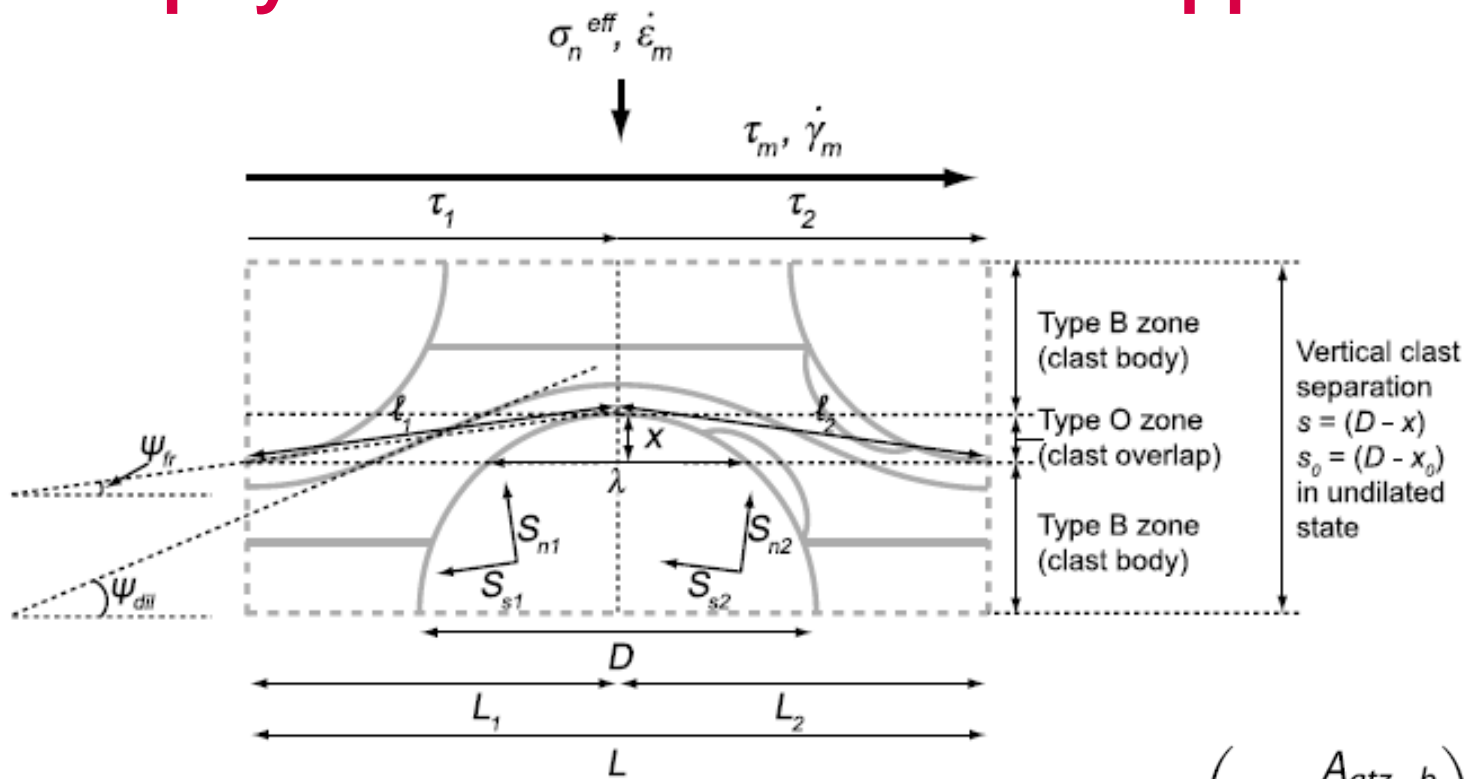
Dilatant deformation:
(1), (2), (3) active

$$\tau_m = \tau_{dil} = \tau_B = \tau_O$$

$$\dot{\gamma}_m = \dot{\gamma}_B + \dot{\gamma}_O + \dot{\gamma}_{dil}$$

Den Hartog & Spiers, JGR, 2014

Microphysical model for matrix-supported gouges



$$\tan \Psi_{fr} = \frac{2(D - x_0)f_{qtz}}{k_f \pi D^2} x$$

$$S_{n1} \ell_1 D = \sigma_n^{eff} L_1 D \cos \Psi_{fr} + \tau_1 L_1 D \sin \Psi_{fr}$$

$$S_{s1} \ell_1 D = \tau_1 L_1 D \cos \Psi_{fr} - \sigma_n^{eff} L_1 D \sin \Psi_{fr}$$

$$\tau_B = \tau_{ph} \left(1 - \frac{A_{qtz-b}}{LD} \right) + \tau_{qtz-b} \frac{A_{qtz-b}}{LD}$$

$$\tau_O = \tau_{ph} \left(1 - \frac{A_{qtz-o}}{LD} \right) + \tau_{qtz-o} \frac{A_{qtz-o}}{LD}$$

$$\tau_{dil} = \left\{ \frac{\tilde{\mu}(1 + \tan^2 \Psi_{fr})}{1 - \tilde{\mu}^2 \tan^2 \Psi_{fr}} \right\} \sigma_n^{eff}$$

Microphysical model for matrix-supported gouges

$$\dot{\gamma}_B = \dot{\gamma}_{qtz-b} = \frac{Al\tau_{qtz-b}\Omega}{RT} \frac{D - 2x}{D(D - x)}$$

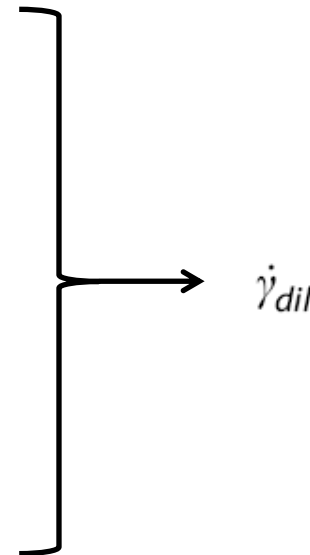
$$\dot{\gamma}_O = \dot{\gamma}_{qtz-o} = \frac{2l\tau_{qtz-o}\Omega}{RT} \frac{1}{\sqrt{Dx - x^2}}$$

$$\dot{\epsilon}_{comp} = \dot{\epsilon}_{dil}$$

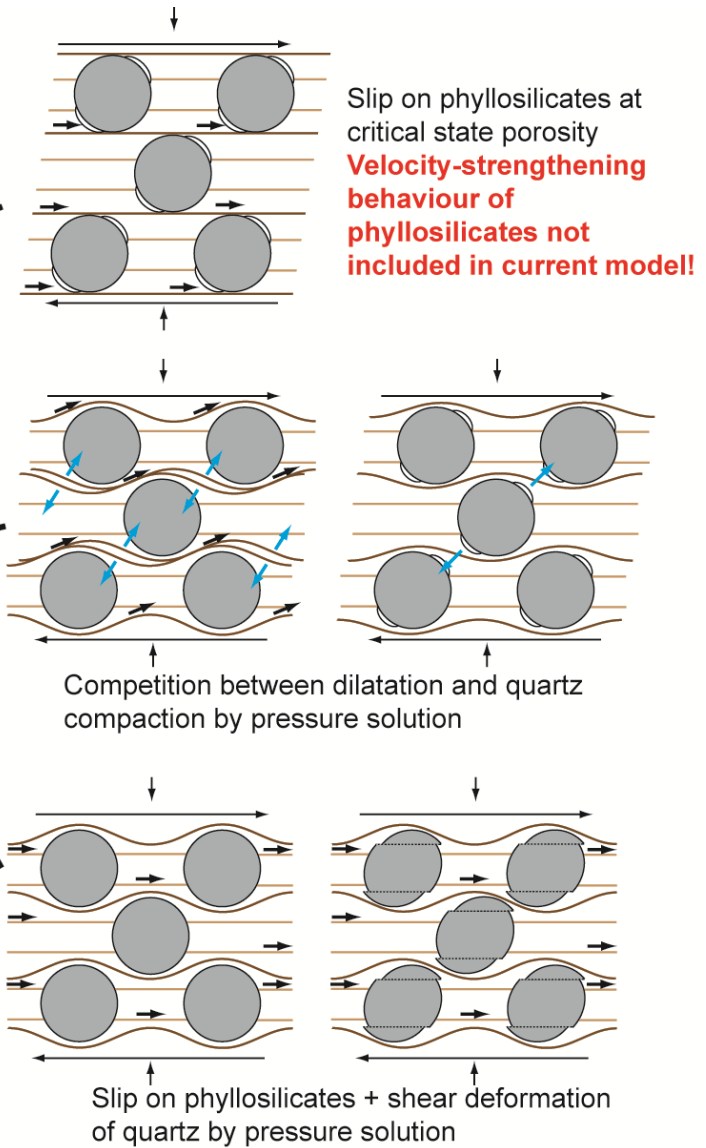
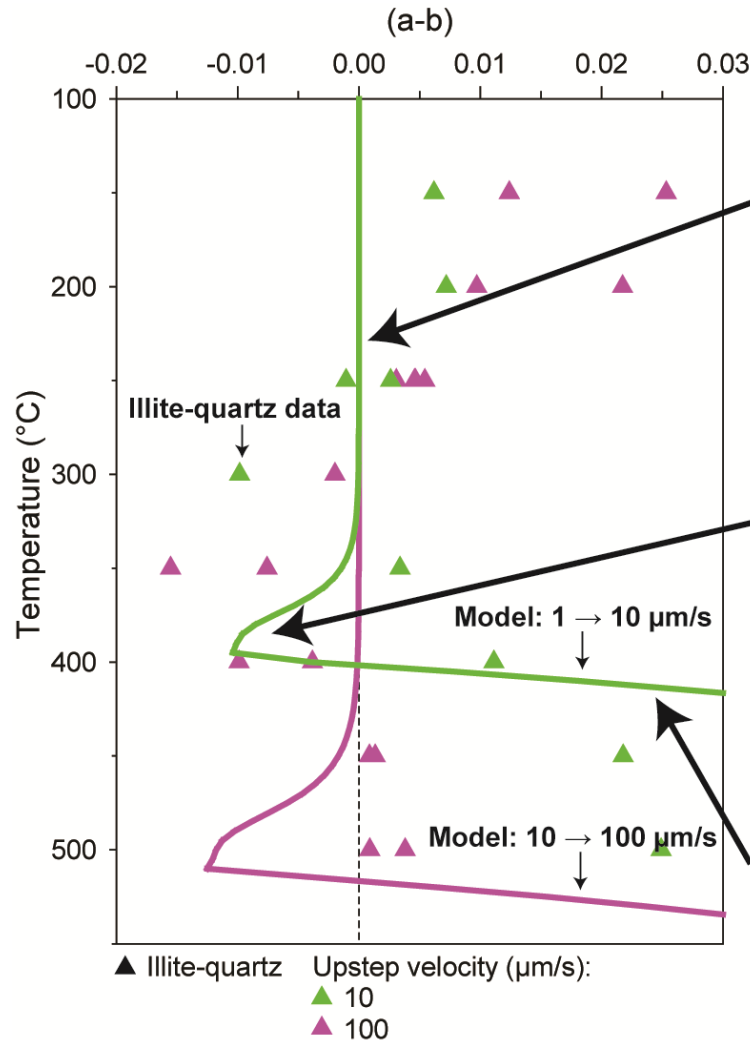
$$\dot{\epsilon}_{comp} = \frac{2l\sigma_n^{eff}\Omega}{RT} \frac{A_{pore}}{(D - x)DL}$$

$$\dot{\epsilon}_{dil} = \left(\frac{d\epsilon_{dil}}{d\gamma_{dil}} \right) \frac{d\gamma_{dil}}{dt} = (\tan\Psi_{dil})\dot{\gamma}_{dil}$$

$$\tan\Psi_{dil} = \left. \frac{\partial[(x/2) \sin(2\pi A_x/L)]}{\partial A_x} \right|_{A_x = 0}$$



Model predictions



Take home messages

1. RSF equations are very useful to describe experimental data and model the seismic cycle.
2. But: RSF equations are empirical equations without a microphysical basis → extrapolation from lab to nature not possible.
3. A microphysical model for friction should account for fluid-rock interactions and the possibility of the presence of a foliation.
4. Microphysical models for the shear deformation of simulated/natural gouges predict a key role of dilatancy + compaction for velocity weakening behaviour (earthquake potential).